C.P. No. 903

C.P. No. 903

MINISTRY OF AVIATION

AERONAUTICAL RESEARCH COUNCIL

CURRENT PAPERS

Wind Tunnel Measurements of the Effect of a Jet on the Time Average and Unsteady Pressures on the Base of a Bluff Afterbody

by

J. E. Rossiter and A. G. Kurn

LONDON: HER MAJESTY'S STATIONERY OFFICE

1967

SEVEN SHILLINGS NET

U.D.C. No. 533.6.048.2 : 533.696.8 : 533.697.4 : 533.6.011.3

C.P. No.903*
August 1965

WIND TUNNEL MEASUREMENTS OF THE EFFECT OF A JET ON THE TIME AVERAGE AND UNSTEADY PRESSURES ON THE BASE OF A BLUFF AFTERBODY

by

J.E. Rossiter

A.G. Kurn

SUMMARY

The time average and unsteady pressures have been measured on the base of a bluff afterbody, containing a single jet, in subsonic and transonic airstreams. Schlieren flash photographs have been used to investigate the mixing process.

It was found that over much of the range of investigation, the mixing of the jet with the external stream was dominated by a vortex motion analogous to the vortex street which occurs behind a bluff two dimensional body. This vortex shedding caused pressure fluctuations on the base of the model and had a significant effect on the time average base pressure.

---

*Replaces R.A.E. Tech. Rep. No.65187 - A.R.C.27495.

CONTENTS

1 INTRODUCTION

Many experimental investigations have been made into the effect of a central jet on the base pressure of a bluff afterbody. Reid and Hastings[1] have studied the case when the external stream is supersonic and have constructed a plausible model of the flow over the base. Further, they have shown that extrapolation is possible from the simpler case of two-dimensional base flow as a function of the base to jet diameter ratio. At subsonic and transonic speeds the picture is more confused and indeed the results of experiments on similar configurations do not agree, as is shown in Ref.2.

During the experiments reported in Ref.2, it was found that at transonic speeds the base pressure varied discontinuously with jet pressure ratio. Further, it was noted that the jet changed abruptly from an unsteady to a steady condition at these discontinuities. This suggested that the time average pressure on the base may be determined, in part at least, by a time dependent flow, in the same way that the pressure on a two-dimensional base is determined by the periodic shedding of vortices. Such a time dependent flow, which might well be sensitive to small differences in configuration, could give rise to the discrepancies referred to above.

In order to investigate the matter further, the tests of Ref.2 have been repeated with a pressure transducer mounted in the base to measure the unsteady component of the pressure.

2 TEST DETAILS

2.1 The tunnel

The tests were made in the 2 ft by 1.5 ft transonic tunnel. This is a variable density facility which, for these tests, was fitted with a working section having longitudinal slots on the roof and floor and solid glass side walls, giving an open area ratio of 6%.

The model was mounted at the end of a long tube passing into the working section from the contraction (Fig.1). The air for the jet was taken from the tunnel settling chamber, through a compressor and drier and delivered through a pipe running along the centre of the model support tube. Pressure and electrical leads were taken away from the model through the annular space between the air delivery pipe and the model support tube.

2.2 The model

The model was the same diameter as the support tube and had a single convergent nozzle in the base (Fig.2). The ratio of nozzle to base area was

0.42. Pressure tappings were provided in the base and at the nozzle exit for the measurement of time average pressures and a pressure transducer was mounted at the position shown in Fig.2 for the measurement of unsteady pressures.

2.3 Instrumentation

H_J, the total head pressure at the centre of the nozzle exit, was deduced from measurements made by a pitot tube positioned in the delivery pipe at 0.75 of the pipe radius from its centreline and 6 ft upstream of the model. This pitot tube had been calibrated, before the tests commenced, by comparison with measurements made at the nozzle exit.

The transducer mounted in the base was of the differential capacity type (R.A.E. type IT-4-37)[3]. It was clamped between rubber pads so that one orifice was flush with the base (see Fig.2) and the other orifice was connected through a length of small bore tubing to one of the pressure tappings on the base. The frequency range was limited by an acoustic resonance at 13 Kc.p.s. in the short length of tube between the transducer and the base of the model. The resonance was well damped and so had little effect on the measured values of the rms of the pressure. However it seems probable that, at the higher jet pressure ratios, significant pressure fluctuations occurred above this frequency so it represents an unfortunate but, as will be seen, not too serious limitation of the experiment.

The transducer was calibrated before each test period by applying a known pressure to it and observing the output from the transducer amplifier on a d.c. voltmeter. Variations in the calibration factor throughout the test were less than ±5%. During the test, the output from the transducer was fed to a Brüel and Kjaer type 2107/2305 frequency analyser set to give an octave selectivity of 40 dB which corresponds to a bandwidth ratio of 11% based on the area under the response curve. With its selective section turned off, the analyser was also used to measure the total rms of the pressure fluctuations. The form of presentation of the unsteady pressure measurements is described in the Appendix.

2.4 Range of investigation

Time average base pressure and amplitude spectra of the unsteady base pressure were measured over a range of jet total head pressure ratios (H_J/H_∞) up to about 3.5 for tunnel Mach numbers (M_∞) of 0.5, 0.7, 0.9, 1.0 and 1.2. The tunnel Reynolds number was held constant at 2.4 million per foot except for $H_J/H_\infty > 3.0$ at $M_\infty = 0.5$ where it was found necessary to reduce the Reynolds number to 1.7 million per foot. In addition amplitude spectra were measured for the same range of H_J/H_∞ with the jet exhausting into still air at a pressure

of 1500 lb/ft^2 for $H_J/H_\infty < 2.3$ and at a pressure of 1000 lb/ft^2 for $H_J/H_\infty > 2.3$. Some schlieren photographs were taken using a flash tube with a time duration of a few micro-seconds.

3 RESULTS

3.1 Conditions at nozzle exit

Because of the small contraction ratio between the supply pipe diameter and the nozzle exit diameter, the total head pressure distribution across the jet was not uniform (see Fig.3). The variation of static pressure near the nozzle exit (p_{N1}) and at a point 2.5 nozzle diameters upstream of the exit (p_{N2}) (see Fig.2) are shown in Fig.4 for $M_\infty = 0$. For isentropic one-dimensional flow in a convergent nozzle, the Mach number upstream of the exit is independent of jet pressure ratio when the exit velocity is sonic i.e. for jet pressure ratios $H_J/H_\infty > 1.89$. However it will be seen from Fig.4 that the pressure ratios, H_J/p_{N2} and H_J/p_{N1} are only constant for jet pressure ratios > 2.0 and 2.4 respectively. This difference between the real flow and an isentropic one-dimensional flow is due to curvature of the sonic surface at the nozzle exit as explained by Herbert and Martlew[4], who show that, in general, the velocity at the periphery and at the centre of a convergent nozzle are quite different, and depend on the curvature of the nozzle wall at exit. For a nozzle having parallel walls at the exit, Herbert and Martlew[4] found that the maximum Mach number of the flow at the periphery of the exit plane was about 1.2 whereas at the centre it was only about 0.85.

Fig.4 also shows that for $H_J/H_\infty < 2.4$, the static pressure at the periphery of the nozzle exit is less than the pressure outside the nozzle. This is shown more clearly in Fig.5 where the ratio p_{N1}/p_B is plotted against H_J/p_B* for the jet with and without external flow (N.B. with no external flow, $p_B = H_\infty$). It will be seen from this figure that the external flow has a significant effect upon the flow within the nozzle. It is thought that this is associated with the periodic shedding of vortices from the bluff annular base which is discussed in para. 4.1.

Measurements of the velocity distribution in the boundary layer on the outside of the model showed that the boundary layer was turbulent and was 0.48 inches thick at M = 0.9 and 0.40 inches thick at M = 1.20.

---

*In this note the jet pressure ratio is in most places described by the ratio H_J/H_∞. However when considering the development of the jet flow, it is sometimes more convenient to use the ratio H_J/p_B since this is the quantity which determines the initial expansion of the jet.

3.2 Time average base pressure

The variation of the time average base pressure with jet pressure ratio for various tunnel Mach numbers is shown in Fig.6. The general shape of the curves is similar for all the subsonic Mach numbers. As jet pressure ratio is increased, the base pressure coefficient first decreases to reach a minimum value of approximately -0.34 when H_J/H_∞ is approximately unity. There is then a small increase in base pressure up to $H_J/H_\infty = 1.5$ followed by a small decrease, although at $M_\infty = 0.9$ the base pressure appears to reach a second minimum for $H_J/H_\infty = 2.5$. At $H_J/H_\infty = 1.4$ for $M_\infty = 0.7$ and 1.55 for $M_\infty = 0.9$, there is an abrupt increase of 0.04 in the value of the base pressure coefficient.

At $M_\infty = 1.0$, the base pressure coefficient continues to decrease through $H_J/H_\infty = 1.0$ and reaches a minimum value of -0.61 at $H_J/H_\infty = 2.0$. It then increases with a discontinuity of 0.07 at about $H_J/H_\infty = 2.57$.

At $M_\infty = 1.2$, the minimum base pressure is -0.56 and occurs at $H_J/H_\infty = 1.25$. There are discontinuities in the curve at $H_J/H_\infty = 1.30$ and 2.40.

For both $M_\infty = 1.0$ and 1.2 there is an initial increase in the base pressure for very low jet pressure ratios.

3.3 Unsteady base pressure

3.3.1 Jet alone

With no external flow, pressure fluctuations were only present on the base of the afterbody when the jet pressure ratio was either above or a little below the critical value ($H_J/H_\infty \doteq 1.89$). The pressure fluctuations comprised a number of periodic (or nearly periodic) components. The frequencies of these components are shown in Fig.7A and it will be seen that the frequency decreases as jet pressure ratio is increased. At any given pressure ratio the frequency of the various components are not harmonically related but approximately lie in a sequence of the form m + 0.25 where m = 1, 2, 3, ..., the curve marked A corresponding to 1.25, that marked B corresponding to 2.25 etc. In general one component has a very much larger amplitude than the others and this has been called the dominant. The magnitude of the pressure fluctuations at the dominant frequency are shown in Fig.7B.

These pressure fluctuations are due to an instability of the jet which has been investigated by Powell[5], by Hammitt[6] and by Davies and Oldfield[7]. Powell has suggested that the instability is due to an aero-accustic resonance in which small disturbances at the jet boundary are amplified as they pass

downstream. At some distance from the nozzle their amplitude is sufficient to give rise to sound waves which are propogated upstream to the nozzle to initiate further disturbances in the jet. The periodic time of a cycle is determined by the time it takes a disturbance to travel downstream in the mixing region plus the time it takes a sound wave to travel upstream from the acoustic source to the nozzle exit. However the relation between the frequency and the jet pressure ratio is not simple for the following reasons:-

(a) the position of the sound source moves downstream as jet pressure ratio is increased and this accounts for the decrease in frequency as jet pressure ratio is increased,

(b) there may be more than one wavelength of the stream disturbance and of the acoustic radiation between the nozzle and the source,

(c) there appears to be a phase difference of one quarter of a wavelength between the stream disturbance and the acoustic radiation so that, for example, the maximum amplitude of the acoustic radiation from the source does not occur until the maximum amplitude of the stream disturbance is one-quarter wavelength downstream of the source. This accounts for the one-quarter which occurs in the ratios of the frequencies of the different components.

3.3.2 Jet with external stream

Fig.8 compares the rms of the unsteady pressure on the base with the time average pressure. It will be seen that the two are intimately related and that in general a decrease in the time average base pressure is accompanied by an increase in the intensity of the unsteady pressure. Of particular interest are the abrupt decreases in the intensity of the unsteady pressure corresponding to the discontinuities in the time average base pressure curves and, at subsonic speeds, the comparatively high value of $\Delta C_{p_{rms}}$ when H_J/H_∞ is approximately unity, corresponding to the minimum value of the time average base pressure.

Typical amplitude spectra of the unsteady base pressure when $M_\infty = 0.5$ are shown in Fig.9. With no jet flow the spectrum is smooth (apart from a small peak at 1300 c/s*,) showing that the pressure fluctuations are random in character. As jet pressure ratio is increased, the spectrum level first falls and then rises. For $H_J/H_\infty = 1.06$ peaks occur in the spectrum showing that, in addition to the random pressure fluctuations, pressure fluctuations at discrete

*This peak occurs in all the amplitude spectra for which the general level is low. It is thought to be due to an acoustic interfence with the tunnel walls since an acoustic wave at this frequency has a wavelength equal to about half the working section height.

frequencies are present. These peaks are first discernible in the spectrum for $H_J/H_\infty \doteq 0.9$. The peak in the rms value at about $H_J/H_\infty = 1$ in Fig.8 is therefore due to both an increase in the random component of the pressure fluctuations and the occurrence of periodic pressure fluctuations. At higher jet pressure ratios ($H_J/H_\infty \doteq 1.61$) the spectrum level falls and the peaks decrease in magnitude. However when the jet is underexpanded ($H_J/H_\infty > 2.0$) large peaks again occur in the spectra and there is a large increase in the random component of the pressure fluctuations.

The frequencies at which the peaks occur in the spectra have been plotted in Fig.8 so that their variation with jet pressure ratio can be compared with the variation in the base pressure. Fig.8 suggests that two distinct types of pressure fluctuation can occur. Firstly, when the jet is underexpanded and $M_\infty = 0.5$ or 0.7, there are pressure fluctuations whose frequency decreases as jet pressure ratio is increased. Secondly, there are pressure fluctuations whose frequency (in general) increases as jet pressure ratio is increased. As will be seen later, the pressure fluctuations in the range of jet pressure ratios from 1.3 to 2.4 at $M_\infty = 1.2$ belong to the second category although their frequency decreases slightly with increasing jet pressure ratio.

The first type of pressure fluctuation comprises a number of periodic components, which are not harmonically related, and is due to the aero-acoustic resonance discussed in section 3.3.1. The frequencies of the pressure fluctuations are modified by the presence of the external stream, since the speed of propogation of the acoustic waves is decreased to a $(1-M_\infty)$ and the position of the acoustic source relative to the nozzle is probably different. A typical schlieren photograph of the flow is given in Fig.10(a) for $M_\infty = 0.5$, $H_J/H_\infty = 3.03$. For this particular condition it would appear that the acoustic source is near the position of the end of the fifth cell in the jet structure and that the sound waves are of opposite phase above and below the jet. Since this is an axi-symmetric jet, it seems probable that the sound wave forms a continuous spiralling surface, a longitudinal section of which is seen in the photograph.

The second type of pressure fluctuation in general comprises a single periodic component although the first overtone is also present for H_J/H_∞ near unity. Excluding for the moment values of $H_J/H_\infty > 1.3$ at $M_\infty = 1.2$, then at any particular value of M_∞, the frequency of the pressure fluctuations increases with jet pressure ratio except for a small range of low pressure ratios where it is almost constant. The pressure fluctuations cease abruptly at some particular value of pressure ratio.

These periodic pressure fluctuations are accompanied by the periodic shedding of vortices from the bluff base as shown by the schlieren photographs of Figs.10 and 11. In most cases the vortices are toroidal in shape (Fig.10(b) and 11(a)) but at $M_\infty = 1.2$ and $1.3 < H_J/H_\infty < 2.4$ the pattern changed erratically from a toroidal to the helical pattern shown in Fig.11(b). Over the range of H_J/H_∞ from 1.3 to 1.68 the flow was so erratic that it was not practical to take readings of the magnitude of the unsteady pressure. Between $H_J/H_\infty = 1.68$ to 2.4 the value in Fig.8(e) are for the helical mode and it will be seen that the frequency of the pressure fluctuations is almost independent of jet pressure ratio whereas for the toroidal mode of vortex shedding the frequency increases with jet pressure ratio. When $H_J/H_\infty > 2.4$ the periodic pressure fluctuations on the base were very weak but were still discernible; the vortex shedding appeared to be in the toroidal mode.

Fig.12 summarises the conditions under which the two types of jet unsteadiness occur. The aero-acoustic resonance only occurs when the external flow is subsonic and, principally, when the jet flow is supersonic although it was discernible for jet velocities slightly less than sonic. The vortex shedding may occur, apparently, under almost any condition for which the aero-acoustic resonance is not present, except for the higher jet pressure ratios with a supersonic external stream. The lowest values of H_J/H_∞ at which the vortex shedding was observed do not necessarily define a lower bound, since the phenomenon may have been present in too weak a form to be discerned by the instrumentation.

4 DISCUSSION

4.1 Comparison with two-dimensional base flow

The schlieren photographs suggest that the vortex shedding in the toroidal mode is similar to that which occurs behind a bluff, two-dimensional body. It is usual to express the frequency of vortex shedding behind a bluff body as a Strouhal number S, defined by:

$$S = \frac{fh}{V_\infty} \qquad (1)$$

where f is the frequency at which vortices are shed from one side of the base

h is the width of the base

and V_∞ is the velocity far ahead of the body.

It has been found from low speed tunnel experiments[8,9,10] that for two-dimensional bodies, S has a value between 0.12 and 0.65 depending on the shape

of the body and the Reynolds number. However Roshko[8,9] has defined a "universal" Strouhal number S* as

$$S^* = \frac{fh'}{V_s} \tag{2}$$

(where h' is the width of the wake behind the body and V_s is the velocity along the separation stream surfaces close to the body)

and has shown that at low speeds S* has a value close to 0.16 for a wide variety of body shapes and for Reynolds numbers, R*, up to ten millions where

$$R^* = \frac{V_s h'}{\nu} \tag{3}$$

Roshko calculates the width of the wake h' by a notched hodograph theory and V_s by assuming that the pressure along the separation stream surfaces is the same as the base pressure.

The flow in the present case differs from that around a two-dimensional bluff base in that, in general, the velocities along the two separation stream surfaces are different. On the separation stream surface from the outer edge of the annular base, the Mach number M_E and velocity V_E may be defined, using Roshko's assumption, by:

$$\left.\begin{aligned} \frac{p_B}{H_\infty} &= \left(1 + 0.2\, M_E^2\right)^{-3.5} \\ \text{and} \quad V_E &= a_E\, M_E \\ \text{where} \quad a_E &= a_o \left(1 + 0.2\, M_E^2\right)^{-0.5} \end{aligned}\right\} \tag{4}$$

and a_o is the speed of sound at tunnel stagnation conditions.

The Mach number M_J and velocity V_J along the separation stream surface from the inner edge of the annular base may be similarly defined as a function of p_B/H_J. Because of the low base pressure, M_E can differ considerably from M_∞ as is shown in Fig.13 in which M_E is plotted against M_J for the range over which toroidal vortex shedding occurs.

Now for each test Mach number M_∞, a condition arises for which $M_E = M_J$ (= M_s say) and, since the total head temperatures of the free stream and jet are the same, $V_E = V_J$. This condition represents the closest analogy to the flow around a two-dimensional bluff base. In Fig.14 a Strouhal number S_s defined by

$$S_s = \frac{fh}{a_s M_s} \qquad (5)$$

is plotted against M_s. The width of the annular base has been chosen as the representative length h, for simplicity, and also because in Nash's experiments on a bluff based aerofoil[11] the wake width did not differ much from the base width for subsonic free stream speeds, corresponding to values of M_s up to 1.6. The frequency f, has been taken as the dominant frequency from Fig.8. On a two-dimensional base the frequency of the pressure fluctuations would be equal to twice the shedding frequency from one side, and this is the reason why the first overtone occurs in Fig.8 when $H_J/H_\infty \doteqdot 1$ i.e. when $V_J \doteqdot V_E$.

At low Mach numbers, S_s has a value very close to Roshko's universal Strouhal number. However this may be fortuitous, since the correct wake width has not been used. When Nash's[11] results from a bluff based aerofoil are calculated on the same basis (see Fig.14) they give a Strouhal number which is rather higher. Nevertheless, the agreement between Nash's results and those of the present test is sufficiently close to justify the conclusion that the vortex shedding phenomenon in the mixing of a jet with an external stream is essentially the same as the vortex shedding behind two-dimensional bluff bases. Apart from the obvious differences between the configurations, it may be significant that the ratio of boundary layer thickness to base width was 1.1 in the present tests but only 0.12 for Nash's tests. Reynolds numbers based on the base width were 0.86×10^5 and 1.7×10^5 respectively.

For the more general case when $V_E \neq V_J$, it has already been noted in connection with Fig.8 that the shedding frequency increases with jet pressure ratio except for very low pressure ratios when it is almost constant. For $M_\infty = 0.5$ and 0.7, the shedding frequency starts to increase when $H_J/H_\infty \doteqdot 1$. This suggests that the frequency depends mainly on whichever is the greater of the two velocities V_E or V_J since $V_E = V_J$ when $H_J/H_\infty = 1$. When $M_\infty = 0.9$, 1.0 and 1.2 the shedding frequency starts to increase for values of H_J/H_∞ less than unity. However this does not necessarily invalidate the hypothesis since, as can be seen from Fig.13, V_E also increases with jet pressure ratio (or M_J) before $H_J/H_\infty = 1$ (or $M_E = M_J$). In Fig.15 a Strouhal number, S, has been plotted against a Mach number, M

where for $V_E > V_J$

$$\left.\begin{aligned} S &= S_E = fh/V_E \\ M &= M_E \end{aligned}\right\} \qquad (6)$$

and for $V_E < V_J$

$$\left.\begin{aligned} S &= S_J = fh/V_J \\ M &= M_J \end{aligned}\right\} \qquad (7)$$

The curve from Fig.14 showing the variation of S_s with M_s for $V_E = V_J$ has also been plotted in Fig.15 and it will be seen that the experimental points lie quite close to this curve. However there is a systematic variation of S which is similar for each value of M_∞ and may well be due to variations in the width of the wake which have not been taken into account.

4.2 Effect of vortex shedding on time average base pressure

It has already been noted that the time average and unsteady base pressures are intimately related. This is perhaps to be expected since not only is the dissipation of momentum in the unsteady wake behind a bluff body associated with its drag, but also the time variations in the wake momentum are associated with the pressure fluctuations on the bluff base. At the conditions when the time average base pressure varies discontinuously with jet pressure ratio, the magnitude of the base pressure with an unsteady wake can be compared with its value when the wake is comparatively steady, so that the increment, ΔC_p, due to the unsteadiness can be deduced. It has been found that the changes in the time average base pressure across the discontinuity are about the same magnitude as the corresponding change in the peak value of the unsteady pressure, as shown in the table below:-

M_∞	H_J/H_∞	ΔC_p	$\Delta C_{p_{rms}}$	$\Delta C_{p_{peak}}$
1.0	2.56	0.075	0.044	0.062
1.2	2.40	0.055	0.040	0.056

Just before the discontinuities, the unsteady base pressure is mainly periodic in character so that the peak values have been deduced from the rms values by assuming a crest factor* of $\sqrt{2}$.

This suggests that the base pressure comprises two components which are combined in the way shown in Fig.16 so that a "steady" base pressure, C_{p_s}, may be postulated such that

$$\left[-C_{p_s}\right] = \left[-C_p\right]_{measured} - \left[\Delta C_p\right]_{peak} \qquad (8)$$

*The crest factor of a periodic function is the ratio of the peak value to the rms value. For a sine wave, the crest factor is exactly $\sqrt{2}$; for a random function of time such as occurs in association with turbulent airflow, the crest factor is usually about 2.5.

It is interesting to speculate as to whether the same argument could be applied throughout the range of jet pressure ratios. Some difficulties are encountered in determining the peak value of the unsteady pressure from its rms value. In general the pressure fluctuations contain both periodic and random components and although the mean square values of these components may be added algebraically, the same is not true of the peak values. However, in order to obtain some idea of how such a postulated steady base pressure varies with H_J/H_∞ and M_∞, Fig.17 has been constructed assuming that the peak values may be added algebraically and that the crest factor is $\sqrt{2}$ for the periodic component and 2.5 for the random component. Ignoring the scatter of the results in Fig.17, which is probably mainly due to the assumptions made in deducing C_{p_s}, the most noticeable feature is that the large discontinuities have been removed from the curves for $M_\infty = 1.0$ and 1.2. In addition it is of interest, that at subsonic speeds, the minima which occurred in the base pressure at $H_J/H_\infty \doteq 1$ (see Fig.6) have been largely eliminated.

It need hardly be stressed that the analysis made in the previous paragraph is purely speculative, but the result does suggest a fruitful field for future research.

5 CONCLUDING REMARKS

As mentioned in the Introduction, the principal aim of this investigation was to find if the time average base pressure was influenced by a time dependent flow in the mixing region of the jet and the external stream. The results show that the base pressure is so influenced, and that the discontinuities observed in the results of Ref.2 are a direct result of a change in the type of mixing flow.

Further, the results show that even when the jet and external streams are supersonic, the mixing may be dominated by vortex shedding. Although the model was not representative of a practical engine installation, the results do suggest a possible additional source of error which could occur when an engine exhaust is simulated by a cold jet in a wind tunnel experiment. The strength and frequency of the vortex shedding will depend on the jet velocity, and this in turn will depend only on the jet temperature for a given value of H_J/H_∞ and nozzle geometry. The contribution to the base pressure from the vortex motion may therefore be seriously in error.

Appendix A

ANALYSIS OF UNSTEADY PRESSURE MEASUREMENTS

The rms of the unsteady base pressure has been made non-dimensional by dividing by the tunnel kinetic pressure, q, to give $\Delta C_{p_{rms}}$.

The amplitude spectra are shown as plots of $p_\varepsilon/q\sqrt{\varepsilon}$ against frequency, f, where p_ε is the rms pressure corresponding to the analyser output in the frequency band εf and ε is the bandwidth ratio of the analyser (= 0.11).

In parts of a spectrum where the ordinate varies slowly with frequency, the ordinate can be related to the power spectral density, F(f), defined by

$$\left(\Delta C_{p_{rms}}\right)^2 = \int_0^\infty F(f)df \qquad (9)$$

so that

$$\left(\frac{p_\varepsilon}{q}\right)^2 = \int_{f(1-\varepsilon/2)}^{f(1+\varepsilon/2)} F(f)df$$

$$\doteq F(f)\varepsilon f$$

since ε is small, and hence

$$\frac{p_\varepsilon}{q\sqrt{\varepsilon}} = \sqrt{fF(f)} \qquad (10)$$

A periodic pressure fluctuation at a discrete frequency appears in the spectrum as a peak having the shape of the analyser response curve. The magnitude of the periodic pressure fluctuation can be extracted from the spectrum by

$$\left[\Delta C_{p_{rms}}\right]^2 = \varepsilon\left[\left(\frac{p_\varepsilon}{q\sqrt{\varepsilon}}\right)_P^2 - \left(\frac{p_\varepsilon}{q\sqrt{\varepsilon}}\right)_R^2\right] \qquad (11)$$

where P refers to the peak

R refers to the spectral level near the peak.

SYMBOLS

$a_E = a_o (1 + 0.2 M_E^2)^{-0.5}$

$a_J = a_o (1 + 0.2 M_J^2)^{-0.5}$

a_o Speed of sound at stagnation temperature of jet and external stream

$a_\infty = a_o (1 + 0.2 M_\infty^2)^{-0.5}$

C_p base pressure coefficient = $(p_B - p_\infty)/q$

f frequency c/s

$F(f)$ power spectral density

h width of base $(= R - r)$

h' width of wake

H_J maximum total head pressure at nozzle exit

H_∞ tunnel total head pressure

$M_E = \{5 ((H_\infty/p_B)^{2/7} - 1)\}^{\frac{1}{2}}$

$M_J = \{5 ((H_J/p_B)^{2/7} - 1)\}^{\frac{1}{2}}$

M_∞ tunnel Mach number

p_B pressure on base

p_{N1} pressure at nozzle exit

p_{N2} pressure in jet supply pipe 2.5 nozzle diameters upstream of exit

p_∞ tunnel static pressure

p_ϵ rms pressure corresponding to voltage passed by frequency analyser

q tunnel kinetic pressure

r radius of nozzle exit

R radius of model

S Strouhal number

$S_E = fh/V_E$

$S_J = fh/V_J$

$S^* = fh'/V_s$

$V_E = a_E M_E$

$V_J = a_J M_J$

V_s velocity along separation streamline

V_∞ tunnel velocity

ϵ bandwidth ratio of frequency analyser

$\Delta C_{p_{rms}}$ rms of unsteady base pressure divided by q

REFERENCES

No.	Author	Title, etc.
1	J. Reid R.C. Hastings	The effect of a central jet on the base pressure of a cylindrical after-body in a supersonic stream. A.R.C. R & M 3224, December 1959
2	A.G. Kurn	A base pressure investigation, at transonic speeds, on an afterbody containing four sonic nozzles and a cylindrical afterbody containing a central sonic nozzle. A.R.C.24932, February 1963
3	W.R. Macdonald P.W. Cole	A sub-miniature differential pressure transducer for use in wind tunnel models. R.A.E. Tech. Note Instn. 169, January 1961
4	M.V. Herbert D.L. Martlew	The design-point performance of model internal-expansion propelling nozzles with area ratios up to 4. A.R.C. R & M 3477, December 1963
5	A. Powell	On the noise emanating from a two-dimensional jet above the critical pressure. Aero Quart. IV (II), 1953
6	A.G. Hammitt	The oscillation and noise of an overpressure sonic jet. J. Aero Sci. 28 pp. 673-684, 1961
7	M.G. Davies D.E.S. Oldfield	Tones from a choked axisymmetric jet. Acustica 12 (4), 1962
8	A. Roshko	On the development of turbulent wakes from vortex streets. NACA TN 2913, March 1953
9	A. Roshko	Experiments on the flow past a circular cylinder at very high Reynolds number. Jour. Fluid Mechanics 10 (3), pp.345-356, 1961
10	N.K. Delany N.E. Sorenson	Low speed drag of cylinders of various shapes. A.R.C.16605, November 1953
11	J.F. Nash V.G. Quincey J. Callinan	Experiments on two-dimensional base flow at subsonic and transonic speeds. A.R.C. R & M 3427, January 1963

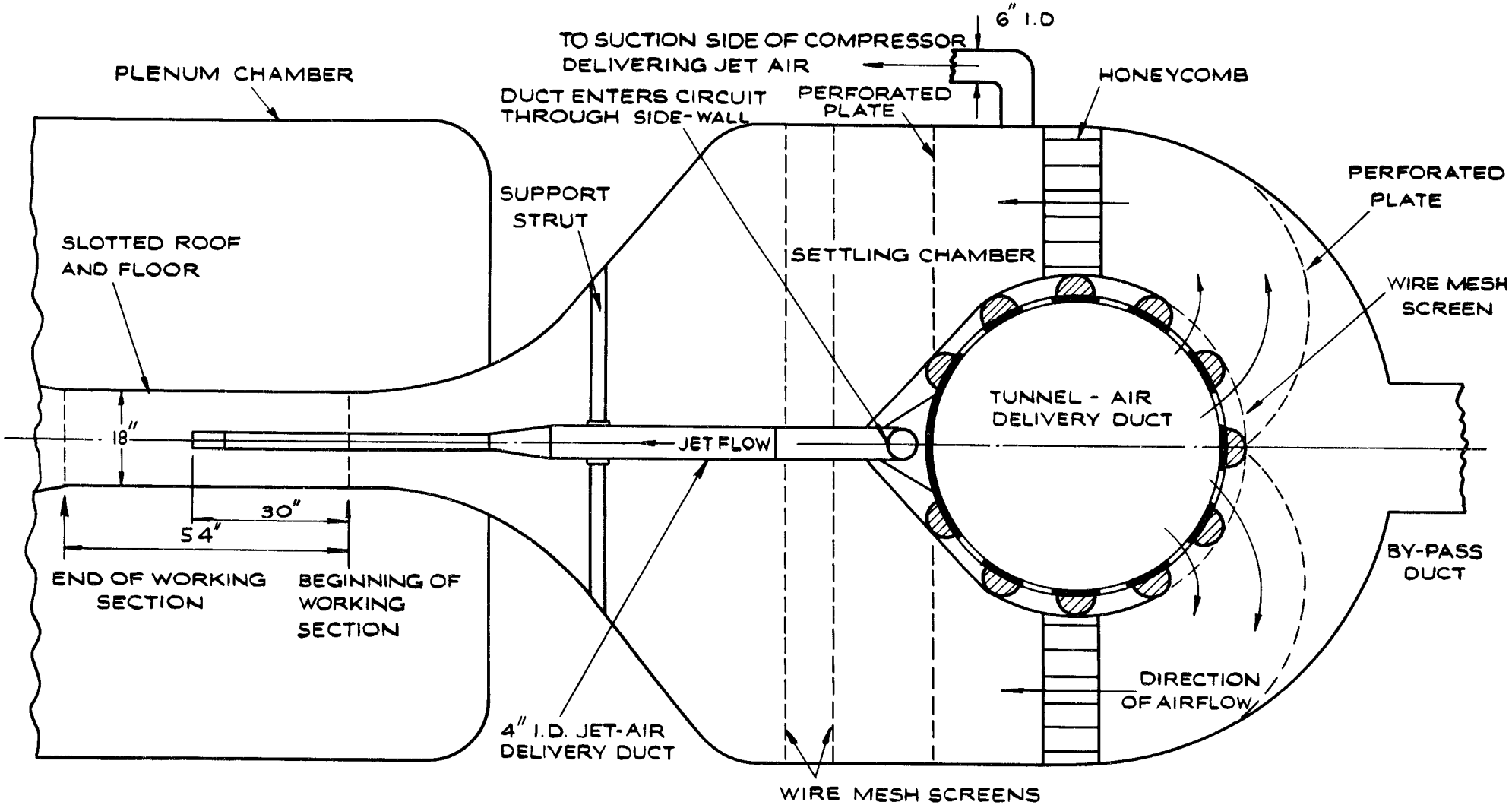

FIG. 1 LINE DRAWING OF $2' \times 1\frac{1}{2}'$ TUNNEL WITH JET RIG INSTALLED

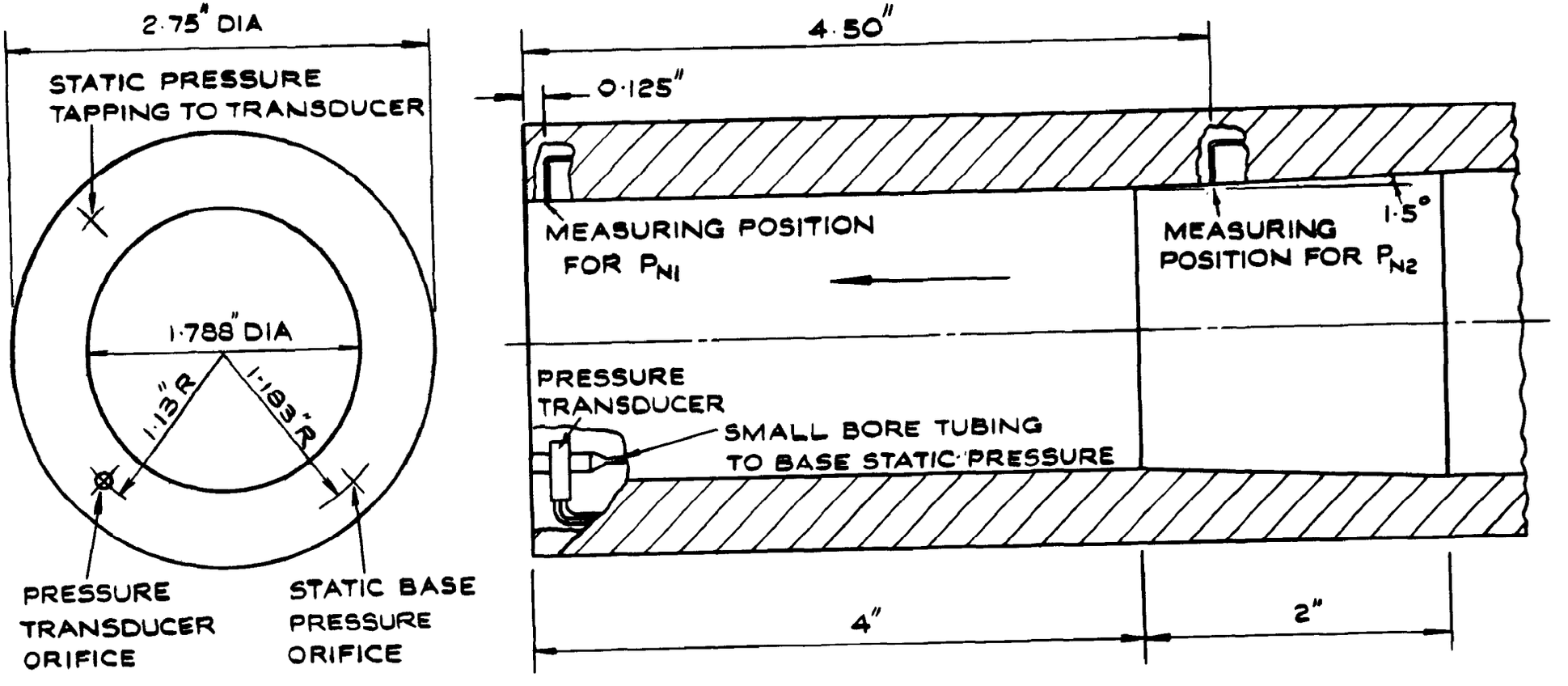

FIG.2 MODEL GEOMETRY SHOWING PRESSURE MEASURING POSITIONS

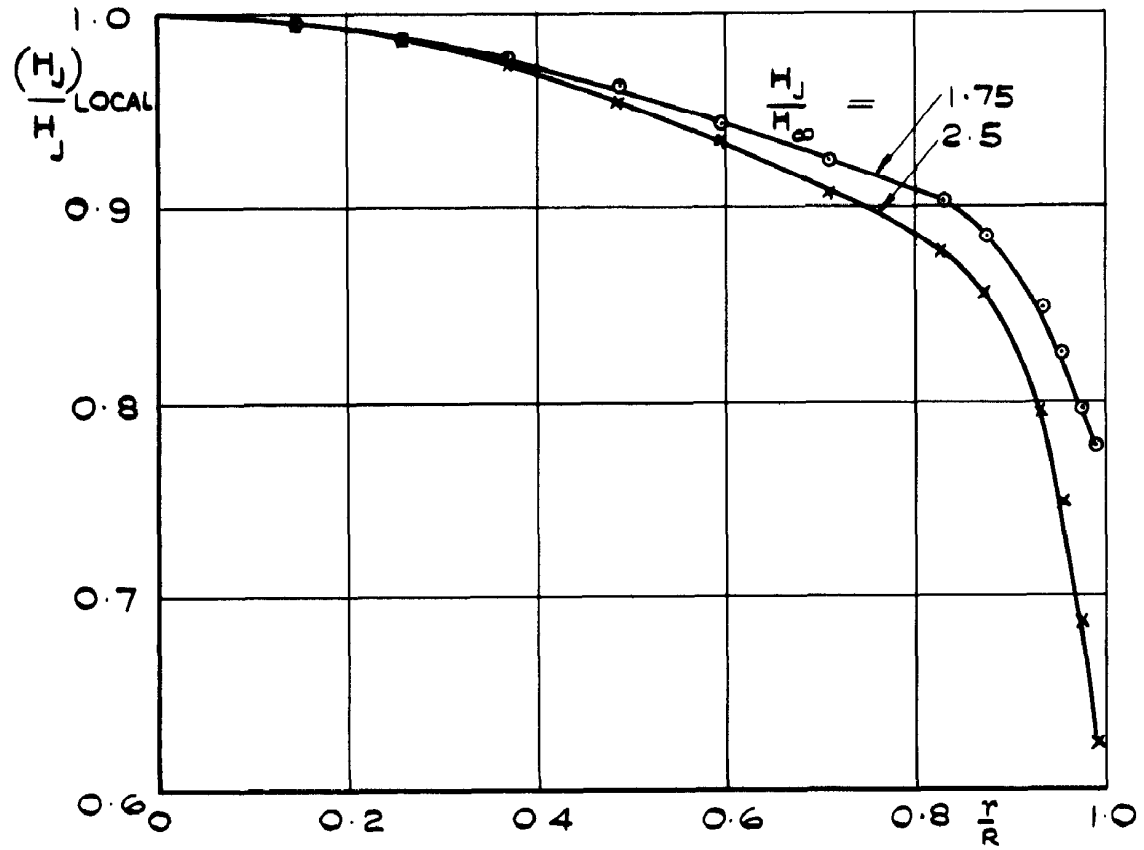

FIG. 3 DISTRIBUTION OF TOTAL PRESSURE AT NOZZLE EXIT $M_\infty = 0$

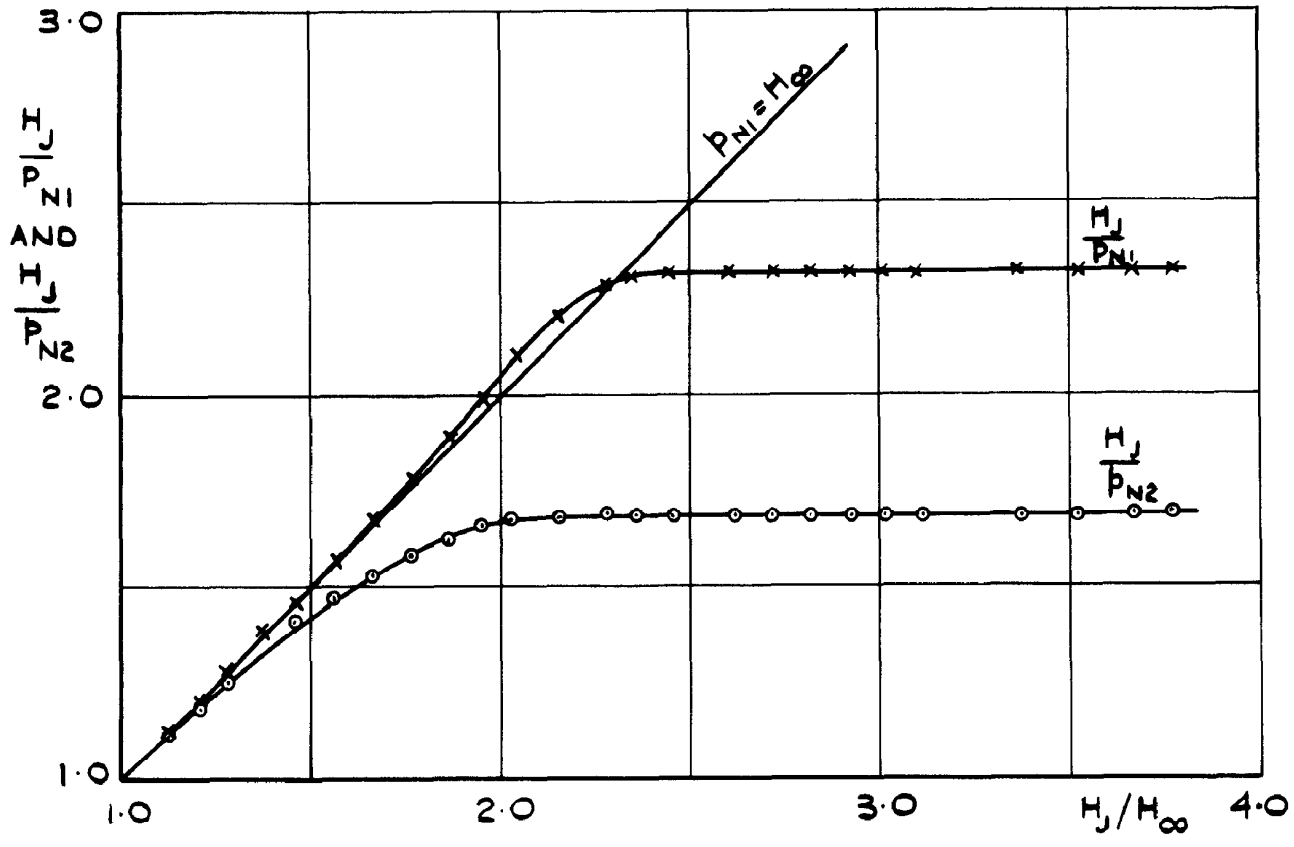

FIG. 4 EFFECT OF JET PRESSURE RATIO ON PRESSURES IN NOZZLE $M_\infty = 0$

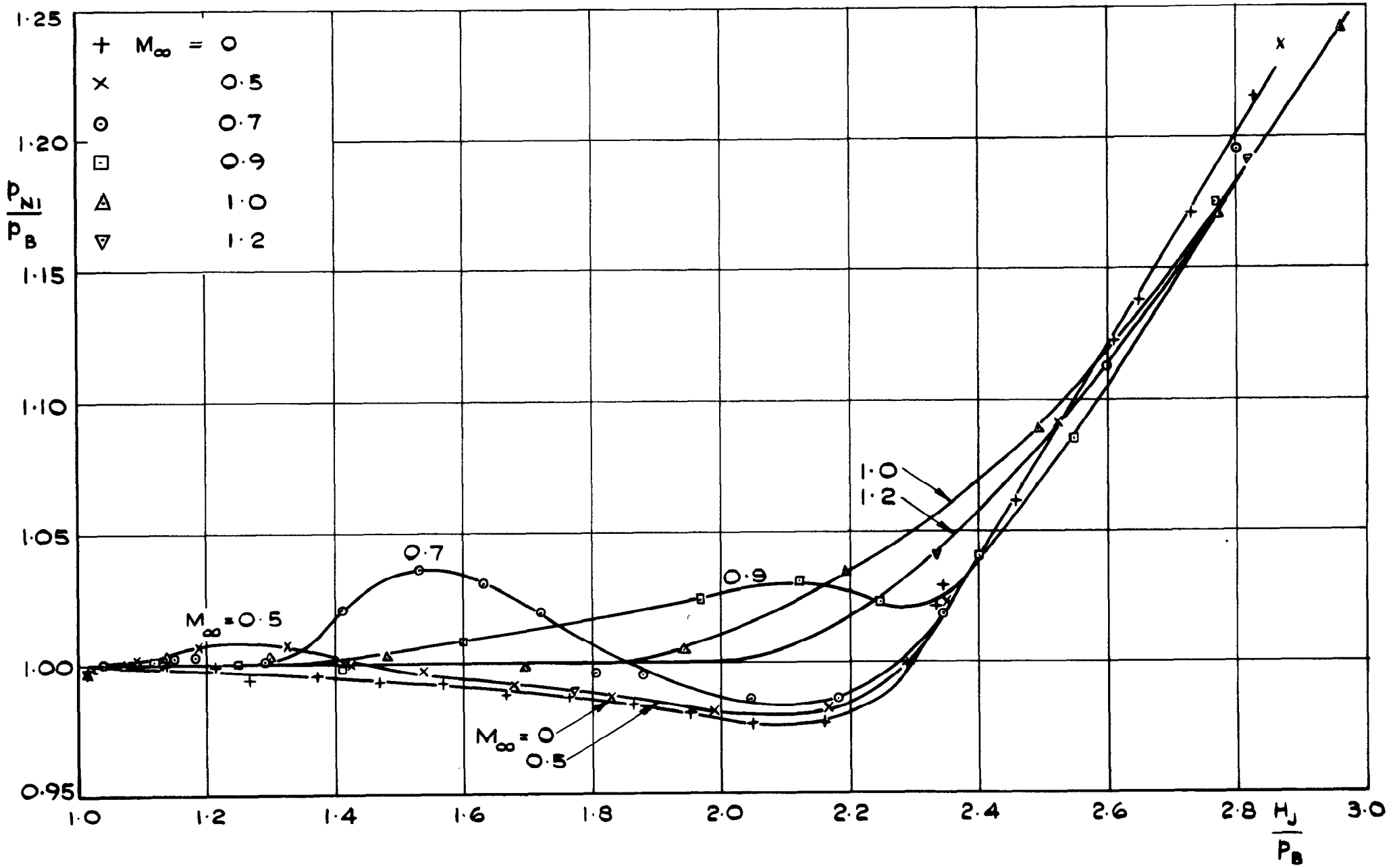

FIG. 5 EFFECT OF EXTERNAL FLOW ON CONDITIONS AT NOZZLE EXIT

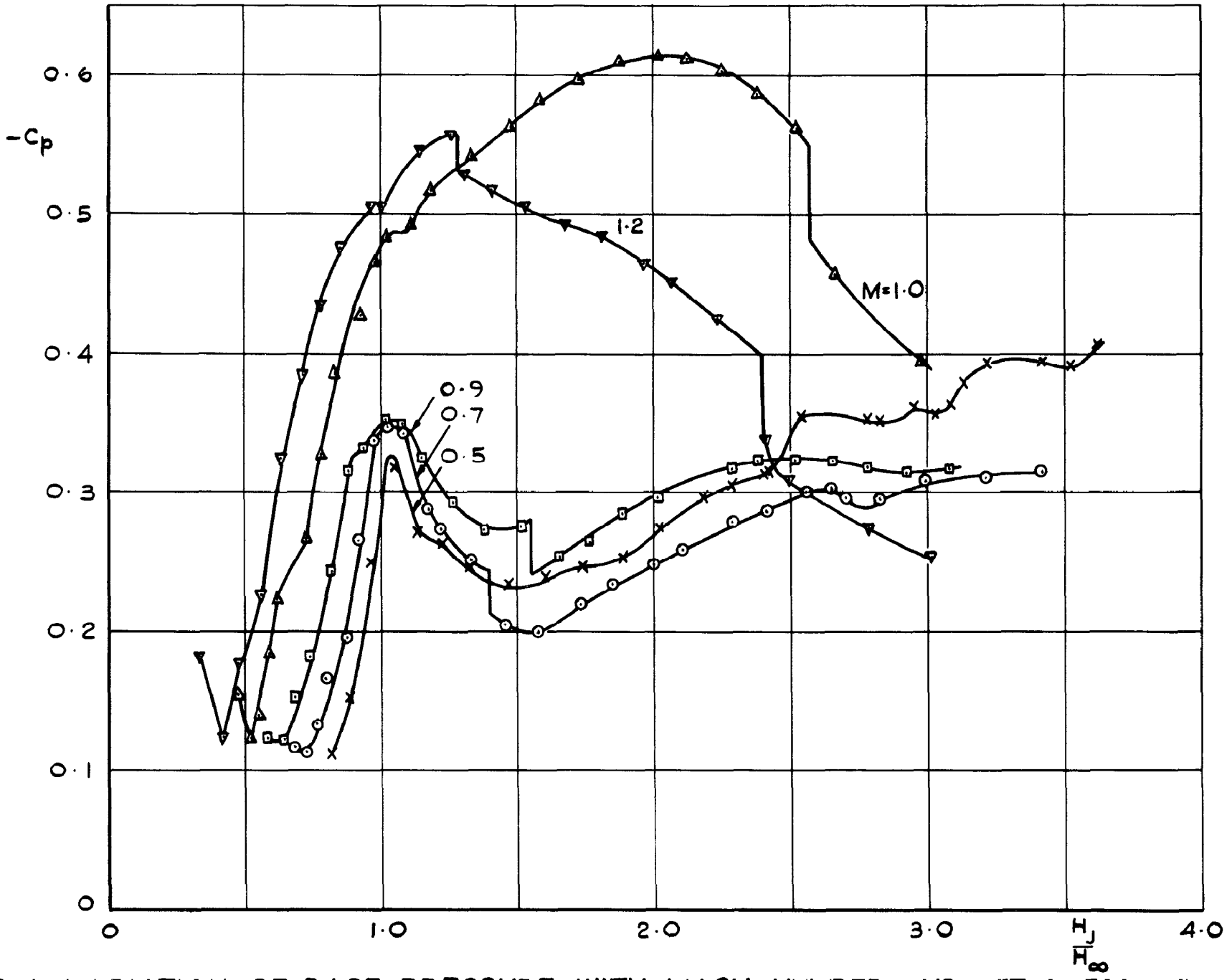

FIG. 6 VARIATION OF BASE PRESSURE WITH MACH NUMBER AND JET PRESSURE RATIO

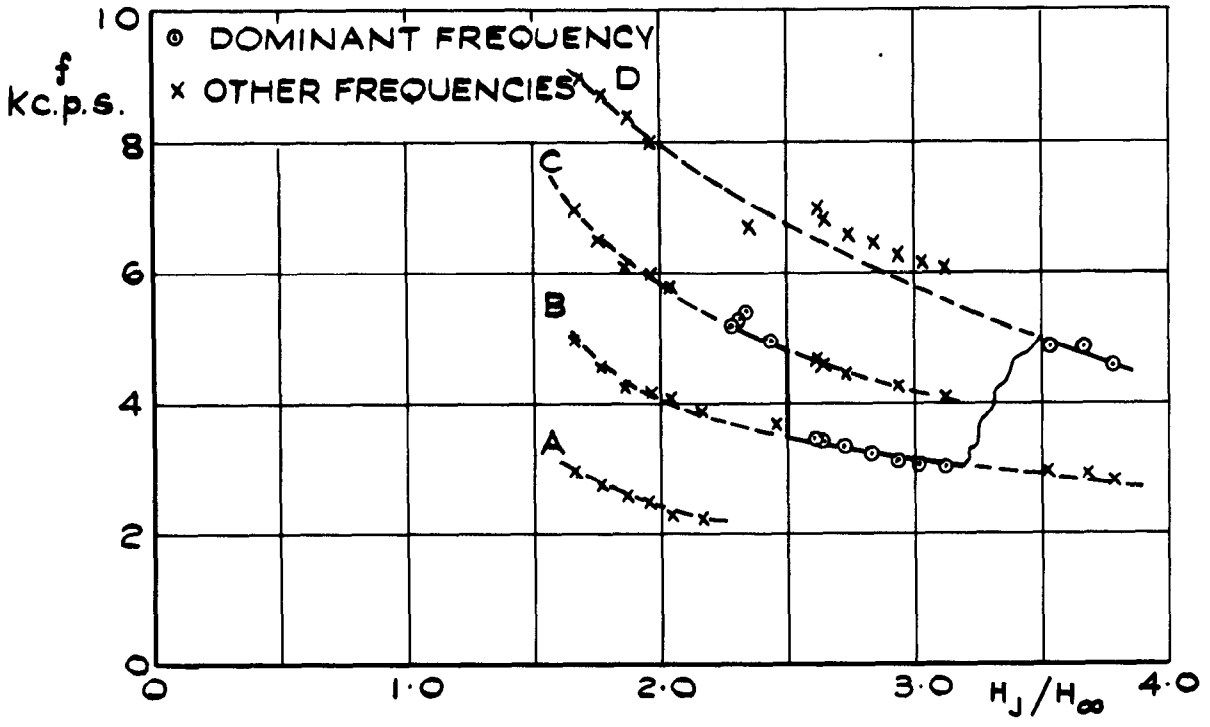

(a) PRINCIPAL FREQUENCIES

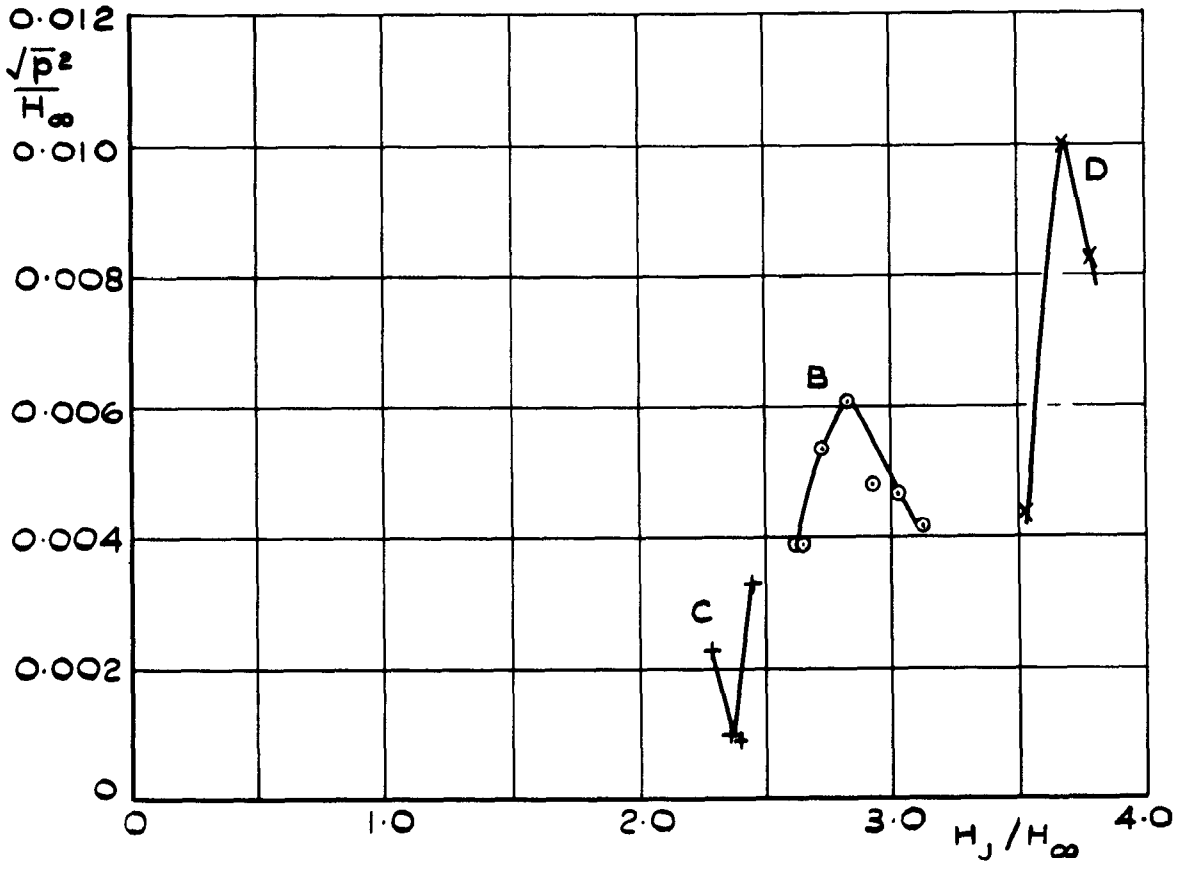

(b) AMPLITUDES OF DOMINANT PRESSURE FLUCTUATIONS

FIG. 7 UNSTEADY PRESSURES ON BASE. JET ALONE

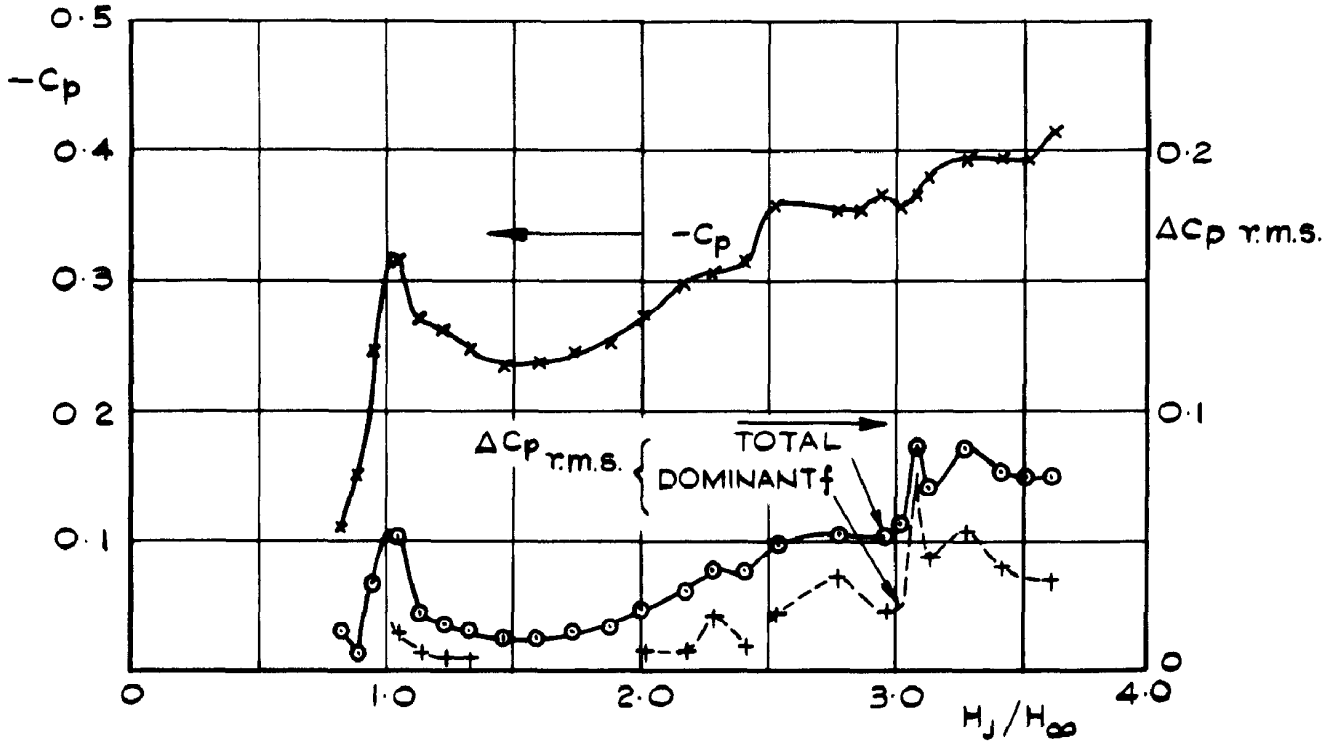

BASE PRESSURES

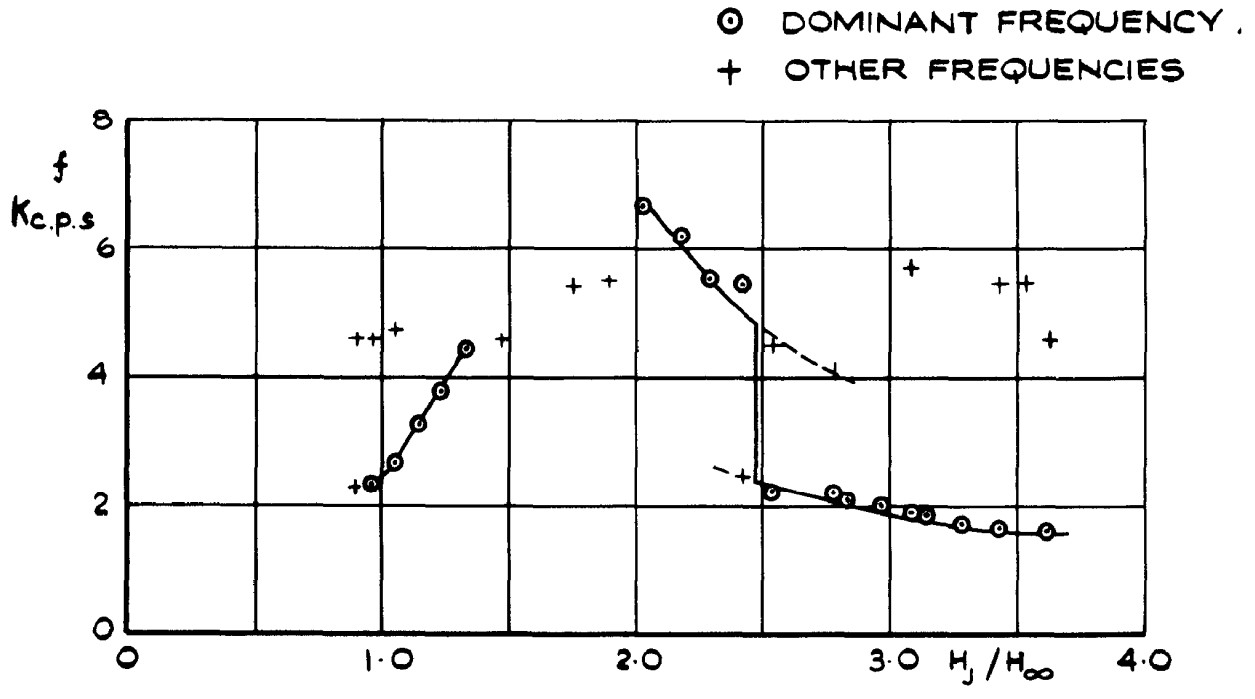

FREQUENCY OF PERIODIC COMPONENTS OF UNSTEADY PRESSURE

FIG. 8 TIME AVERAGE AND UNSTEADY BASE PRESSURES

(a) $M_\infty = 0.5$

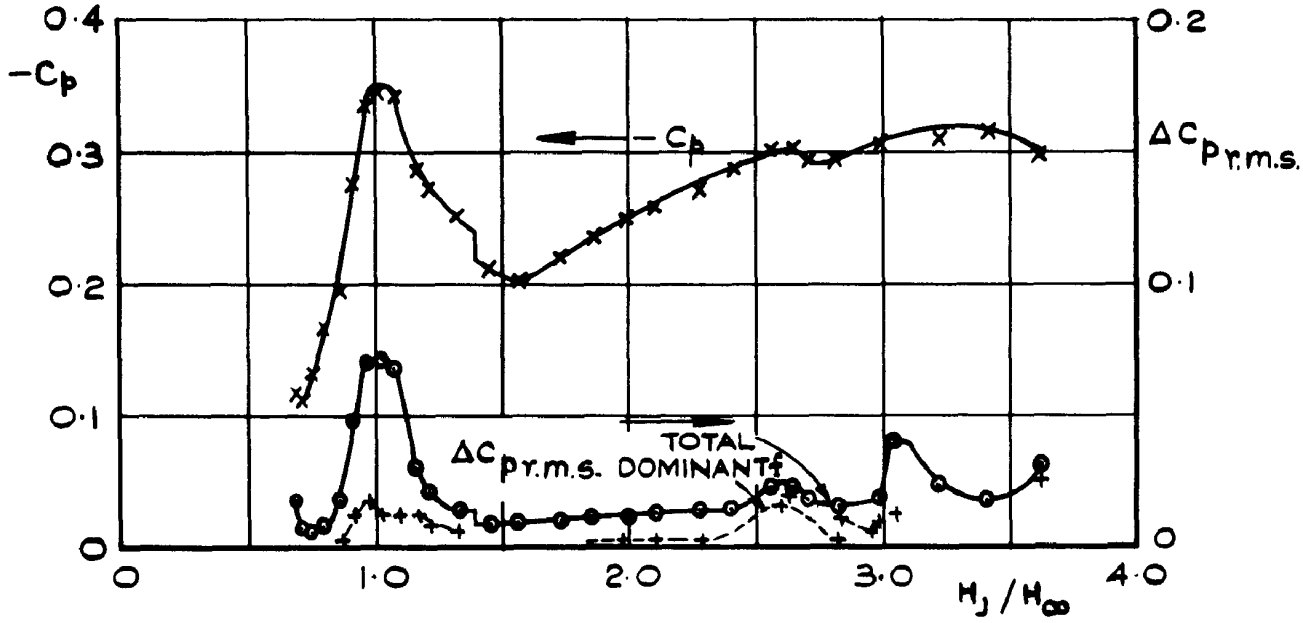

BASE PRESSURES

⊙ DOMINANT FREQUENCY

\+ OTHER FREQUENCIES

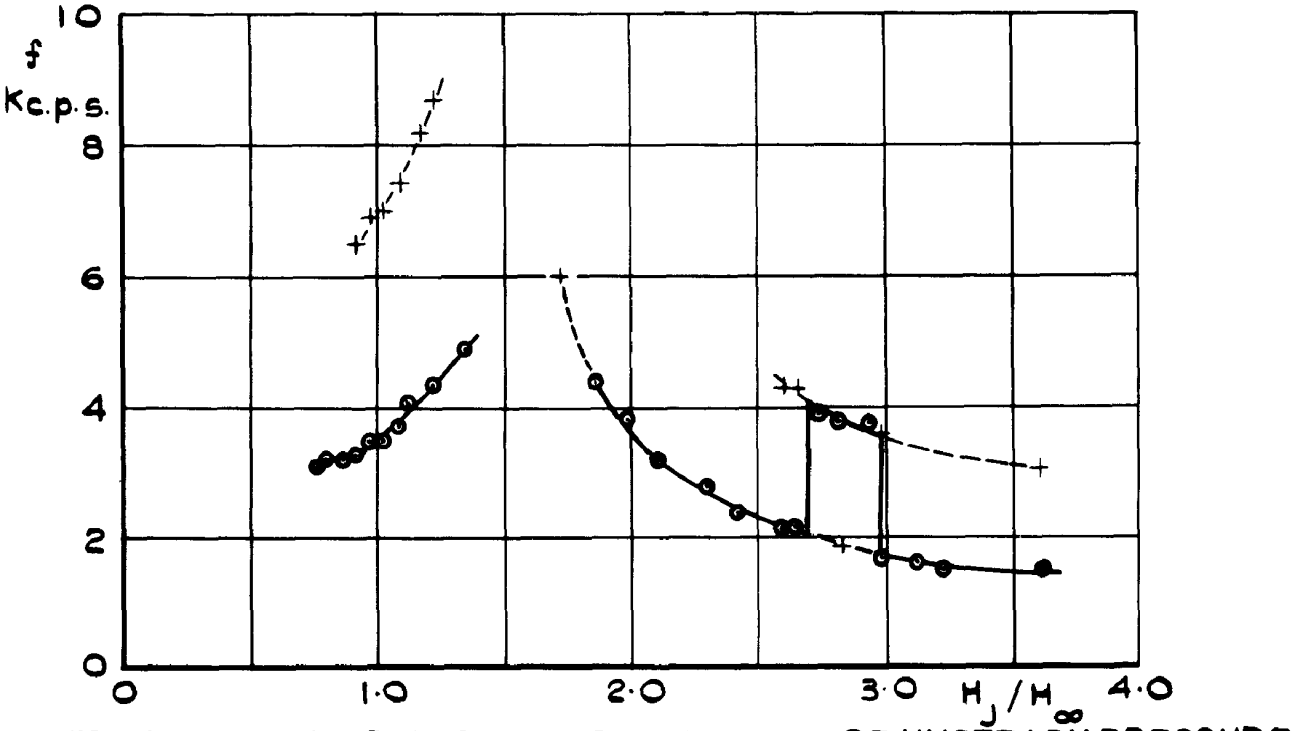

FREQUENCY OF PERIODIC COMPONENTS OF UNSTEADY PRESSURE

FIG. 8 (CONT'D) TIME AVERAGE AND UNSTEADY BASE PRESSURES

(b) $M_\infty = 0·7$

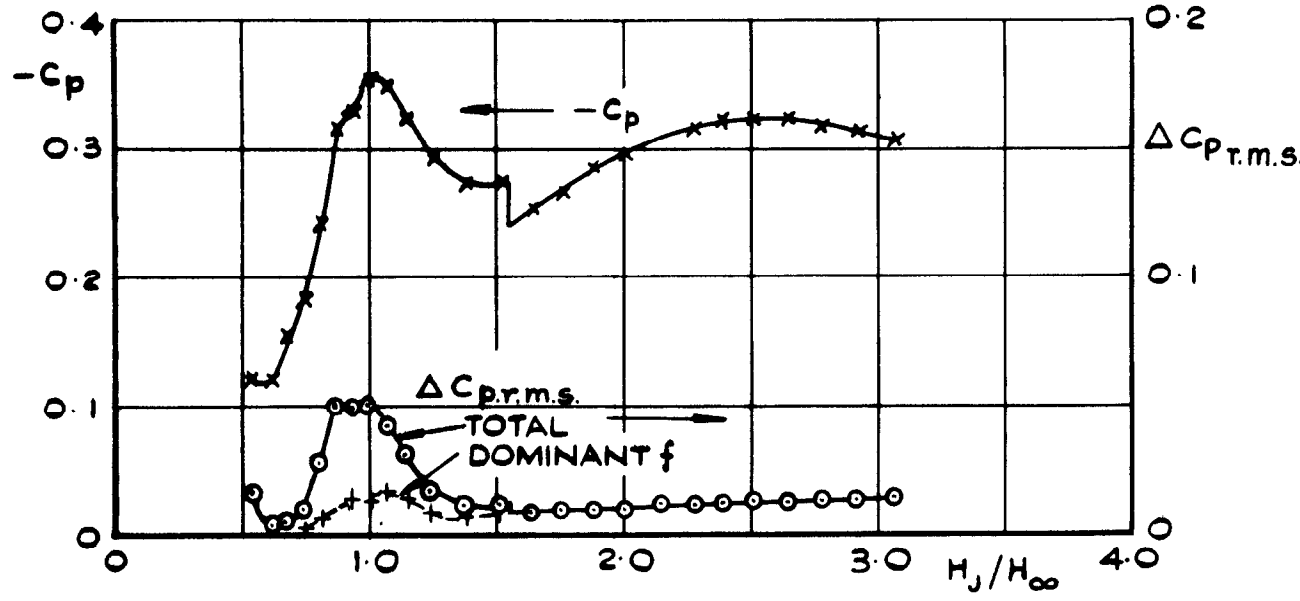

BASE PRESSURE

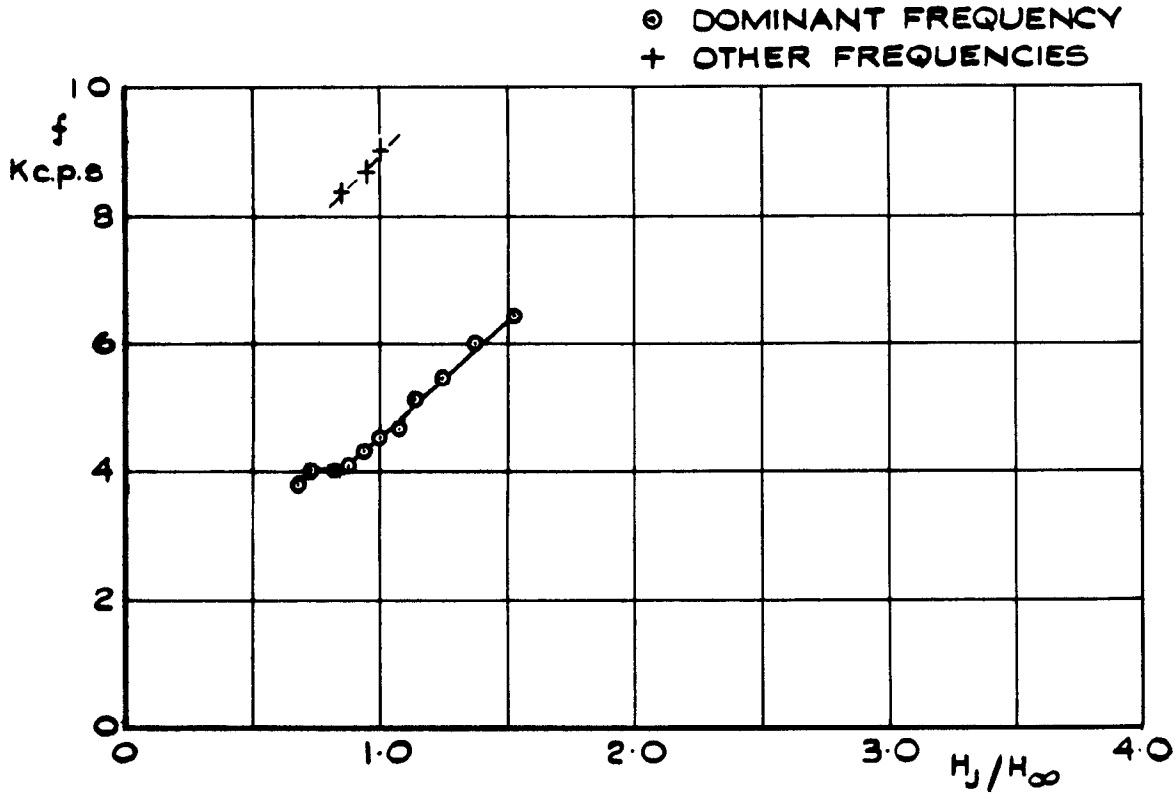

FREQUENCY OF PERIODIC COMPONENTS OF UNSTEADY PRESSURE

FIG.8 (CONT'D) TIME AVERAGE AND UNSTEADY BASE PRESSURES

(c) M=0·9

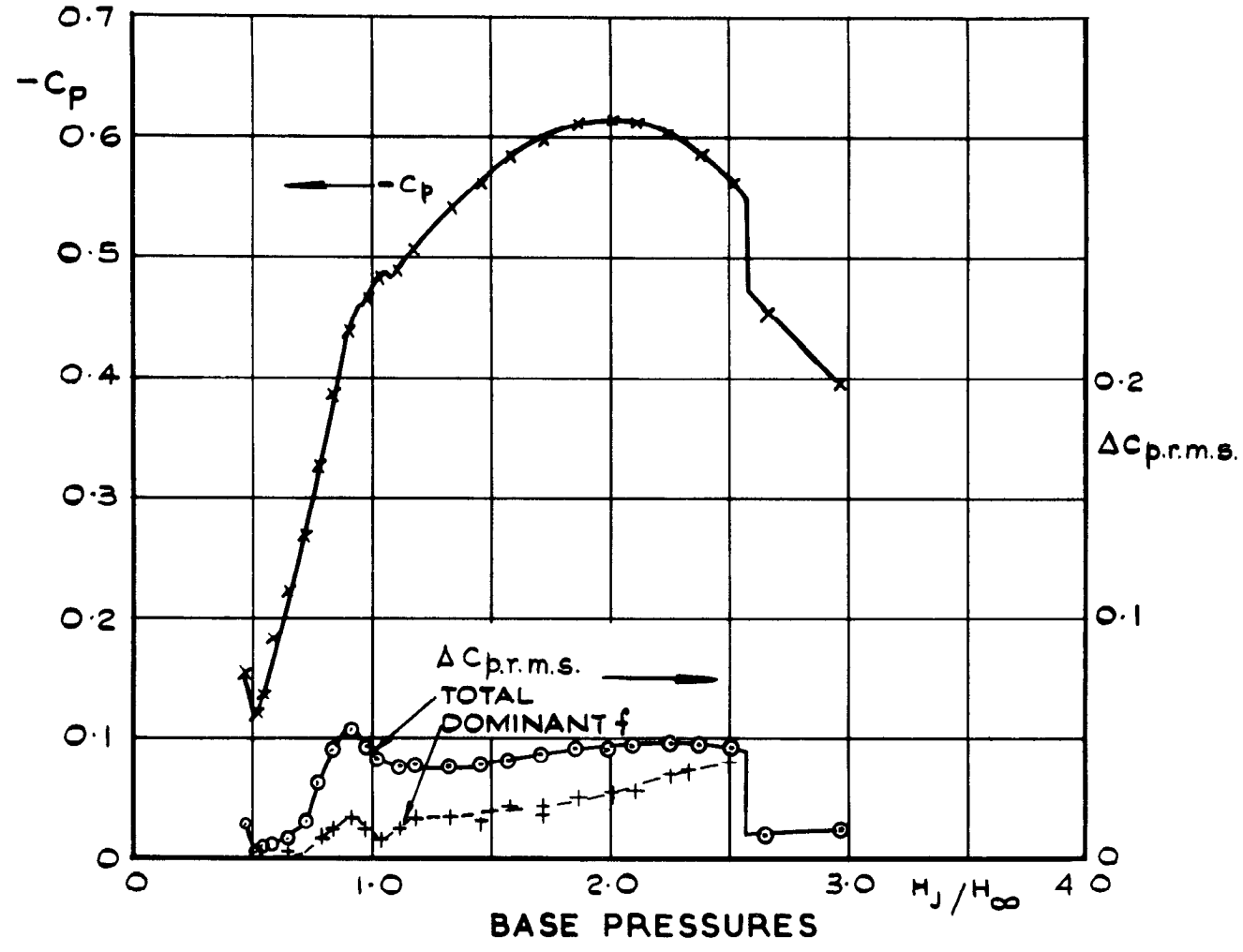

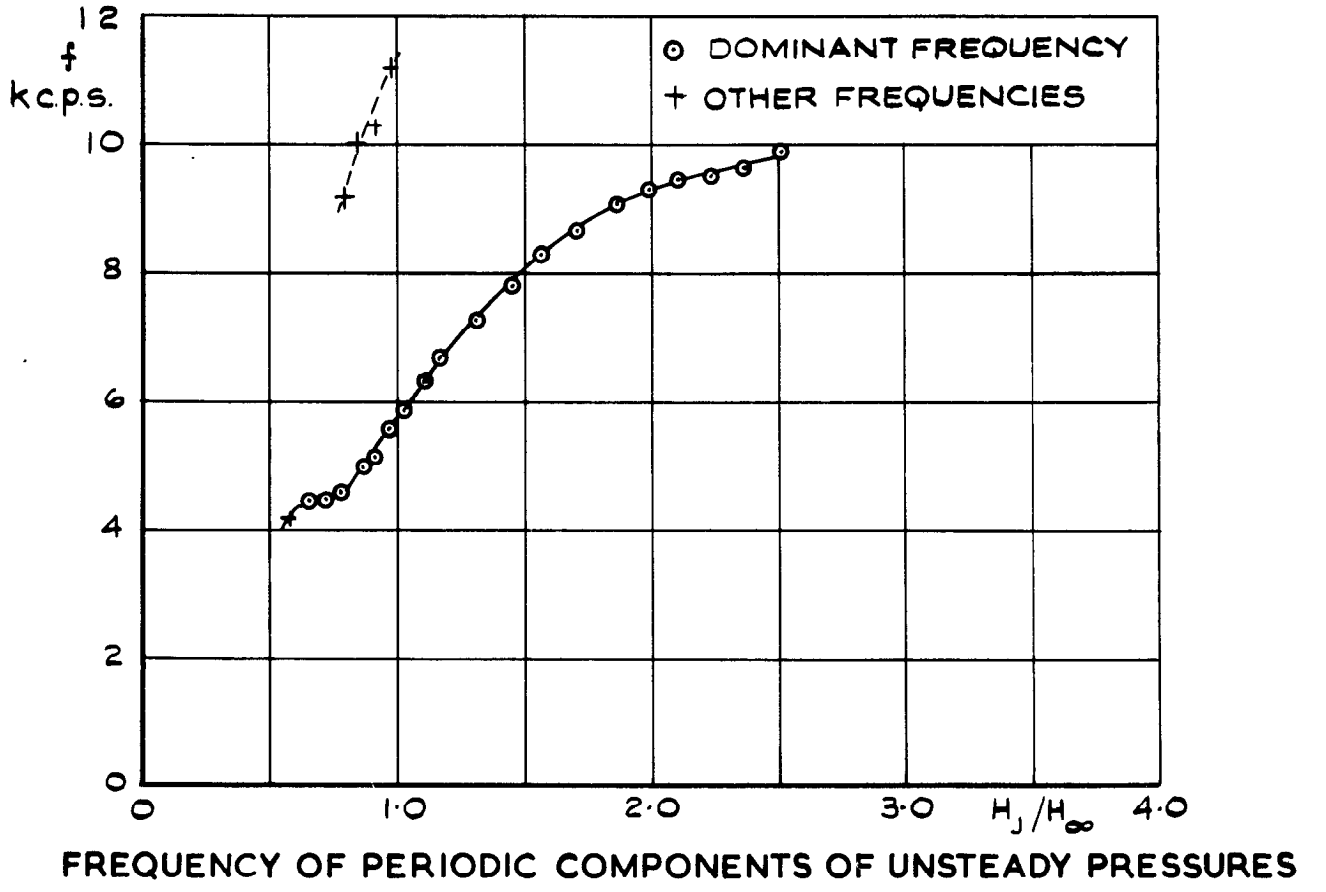

FIG. 8 (CONT'D) TIME AVERAGE AND UNSTEADY BASE PRESSURES
(d) $M_\infty = 1·0$

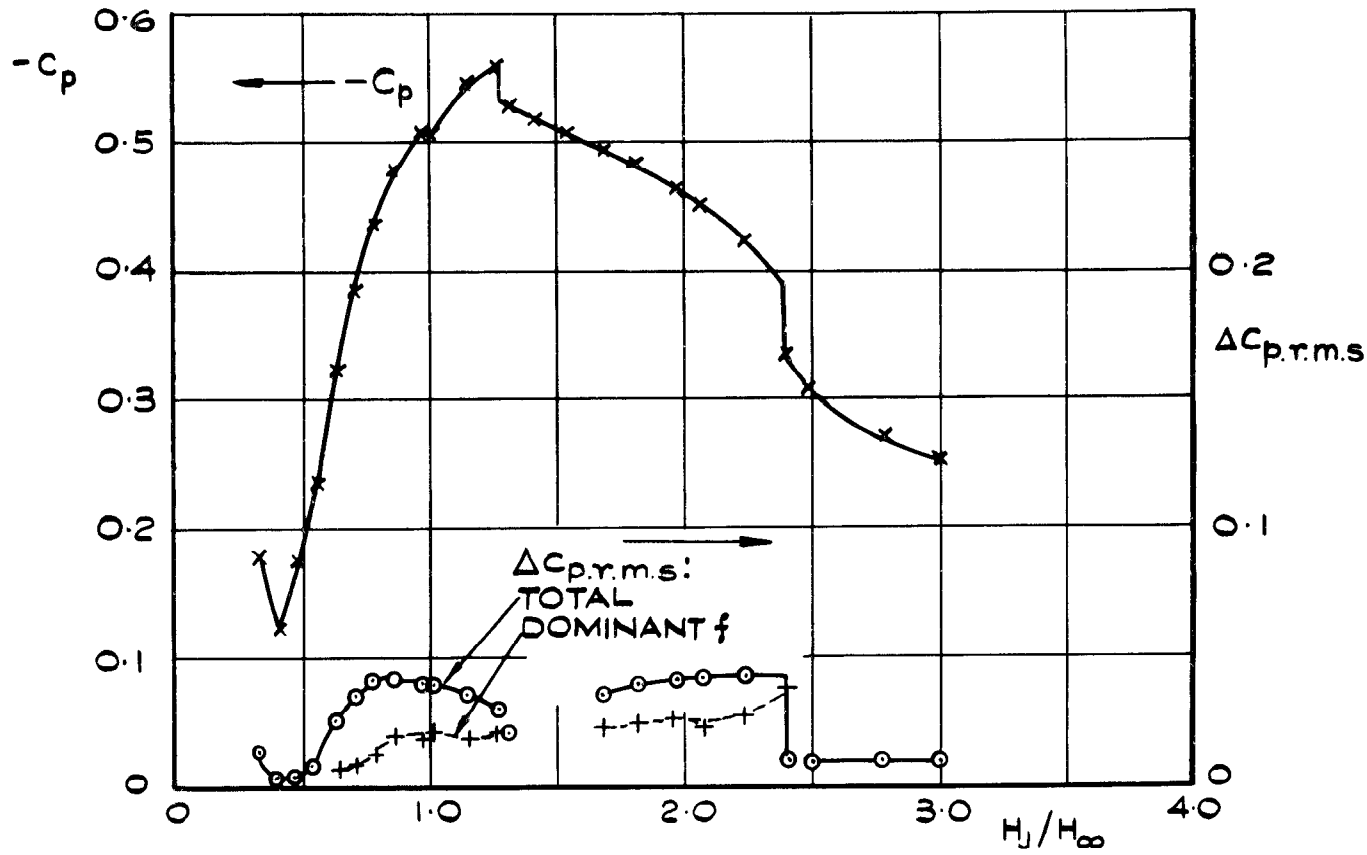

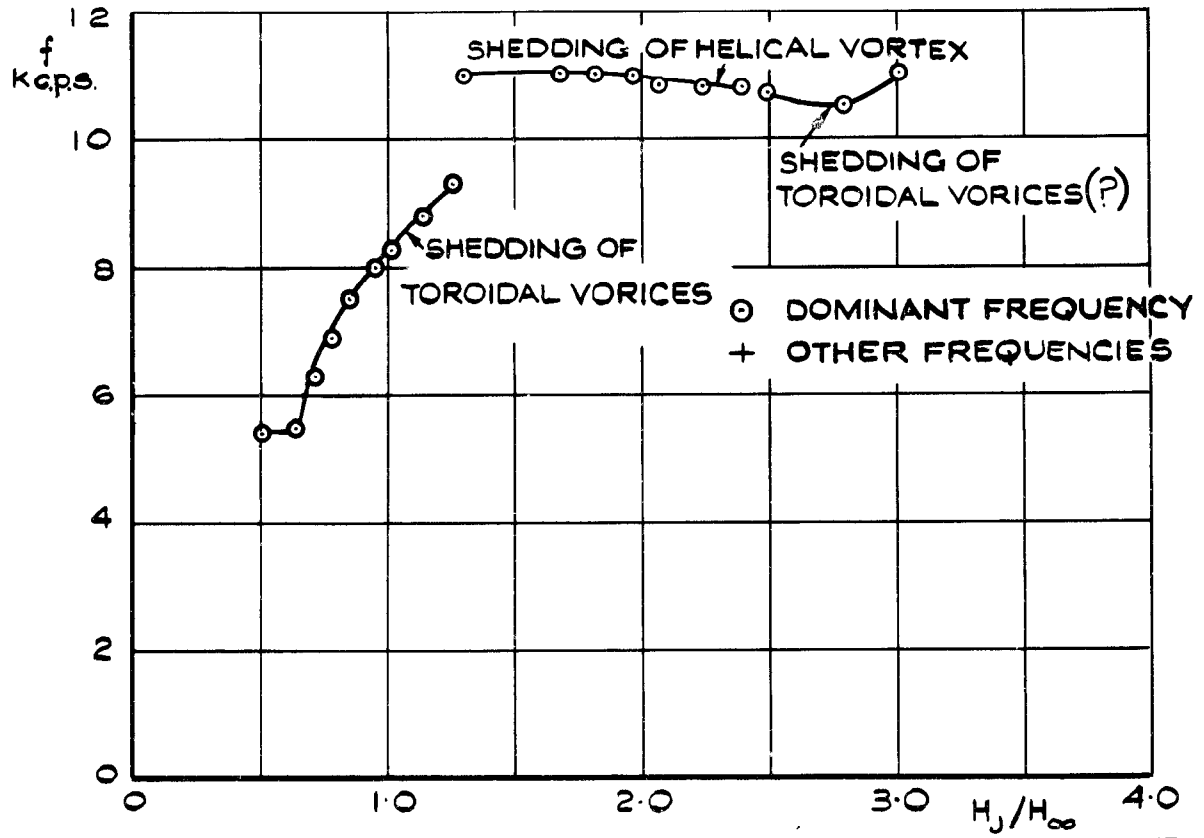

FREQUENCY OF PERIODIC COMPONENTS OF UNSTEADY PRESSURE

FIG.8 (CONCL'D) TIME AVERAGE AND UNSTEADY BASE PRESSURE

(e) $M_\infty = 1 \cdot 2$

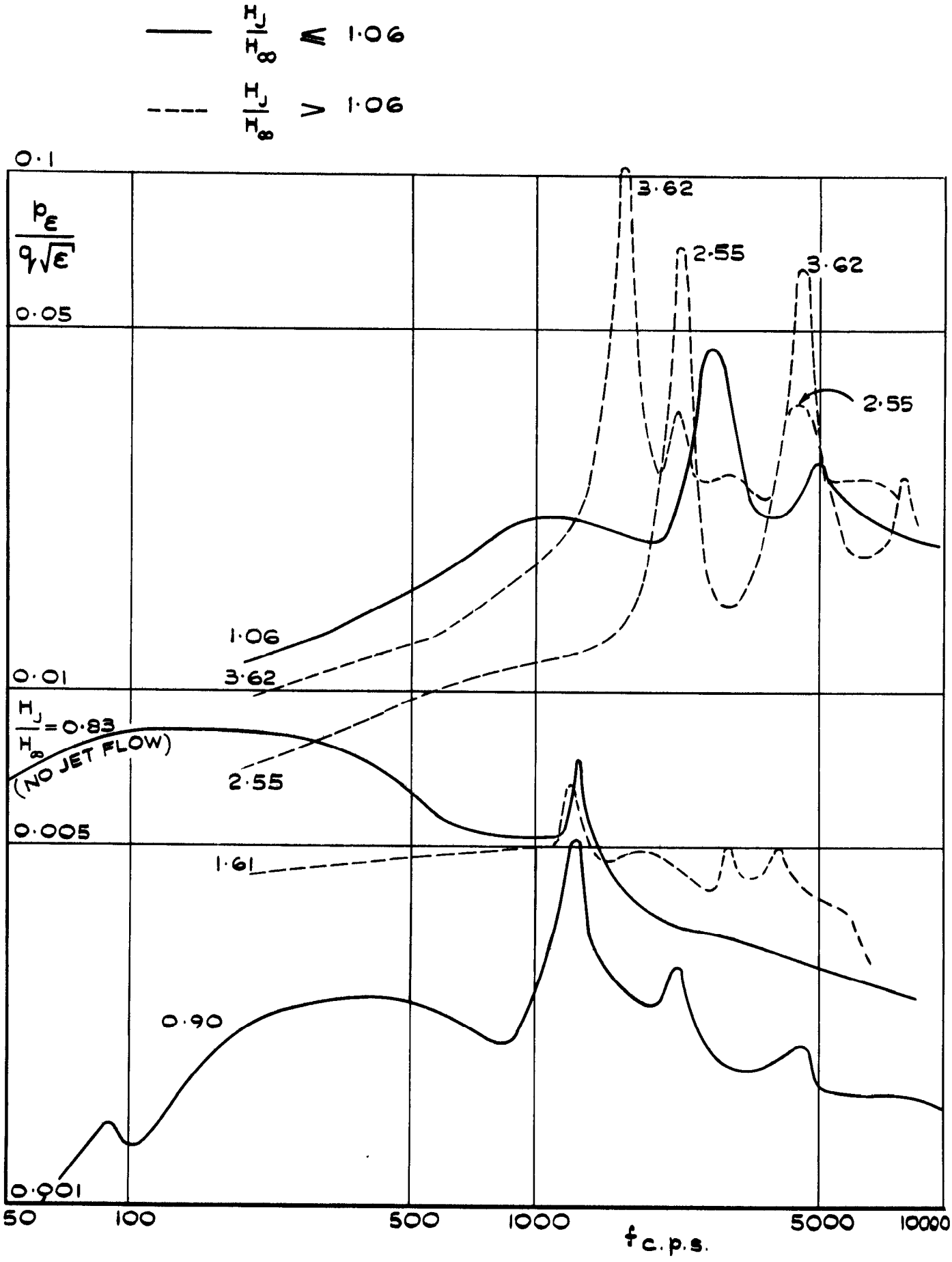

FIG. 9 TYPICAL AMPLITUDE SPECTRA OF UNSTEADY BASE PRESSURE

$M_\infty = 0 \cdot 5$

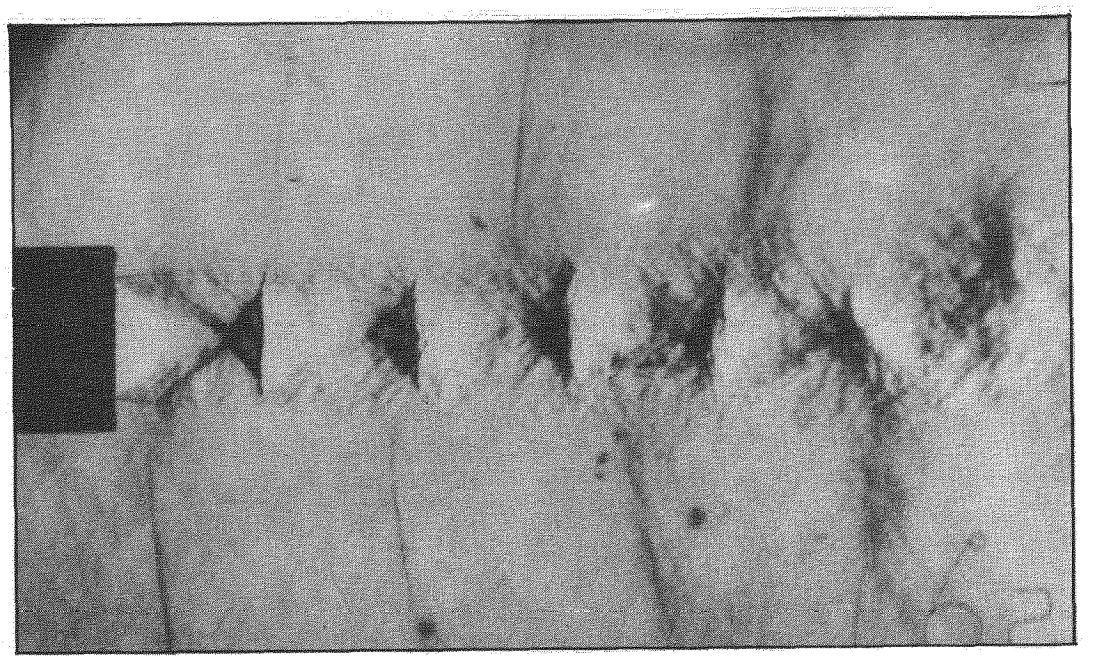

(a) Aero—acoustic instability. $H_J / H_\infty = 3.03$

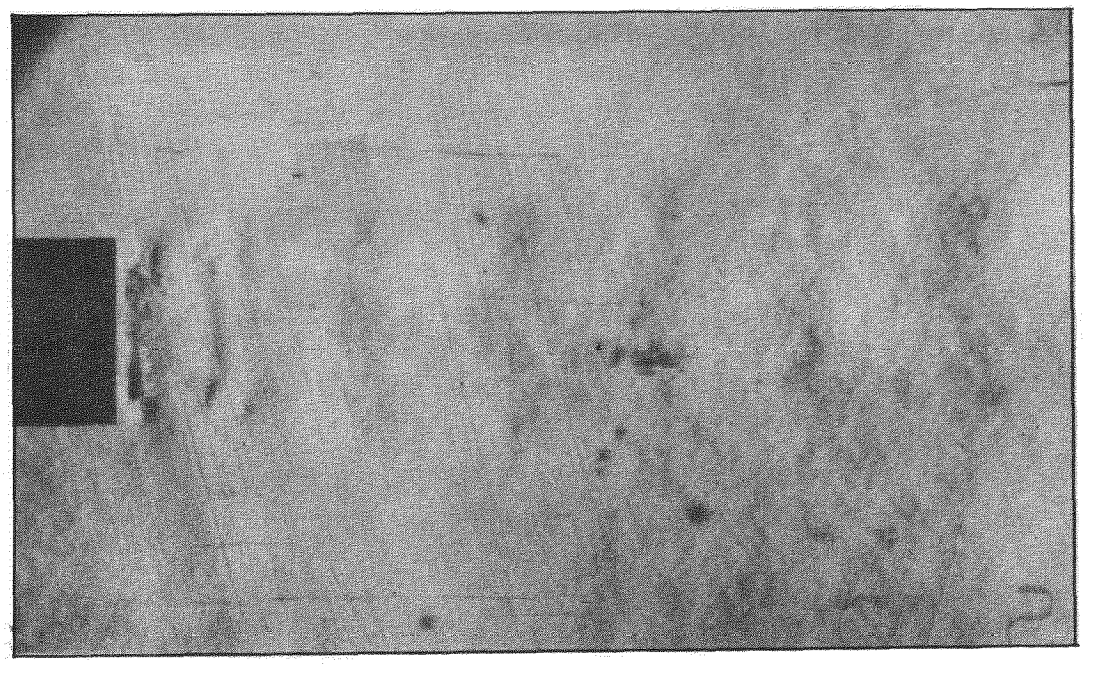

(b) Toroidal vortex shedding. $H_J / H_\infty = 1.06$

Fig.10. Schlieren photographs. $M_\infty = 0.5$. K.E. vertical

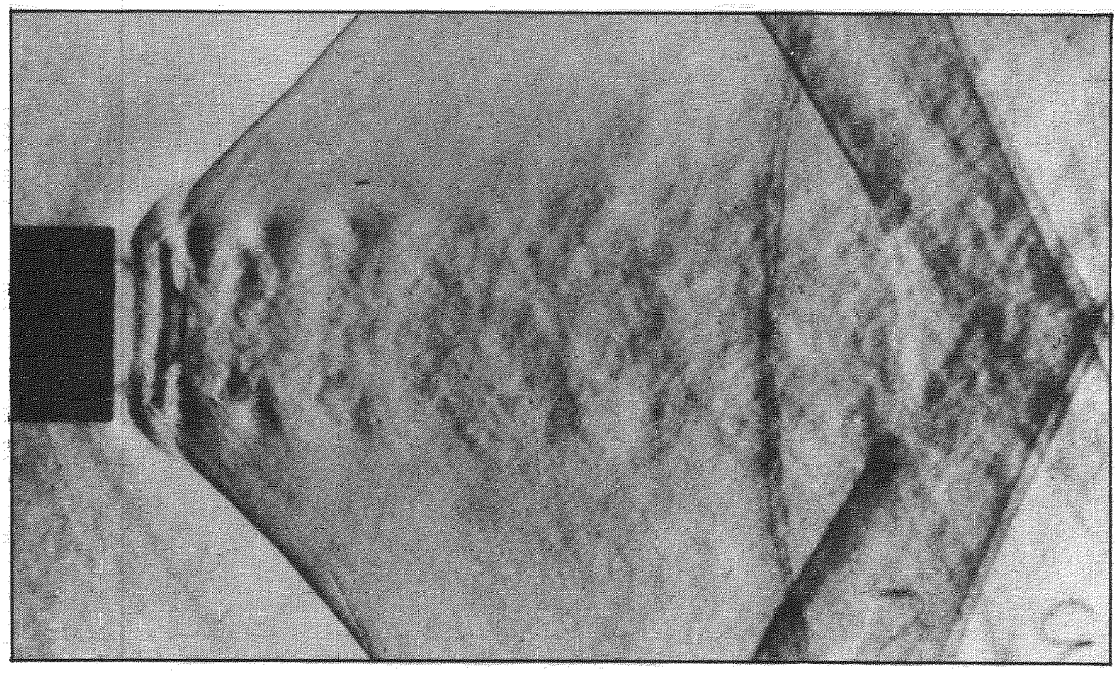

(a) Toroidal vortex shedding. $H_J / H_\infty = 1.10$.

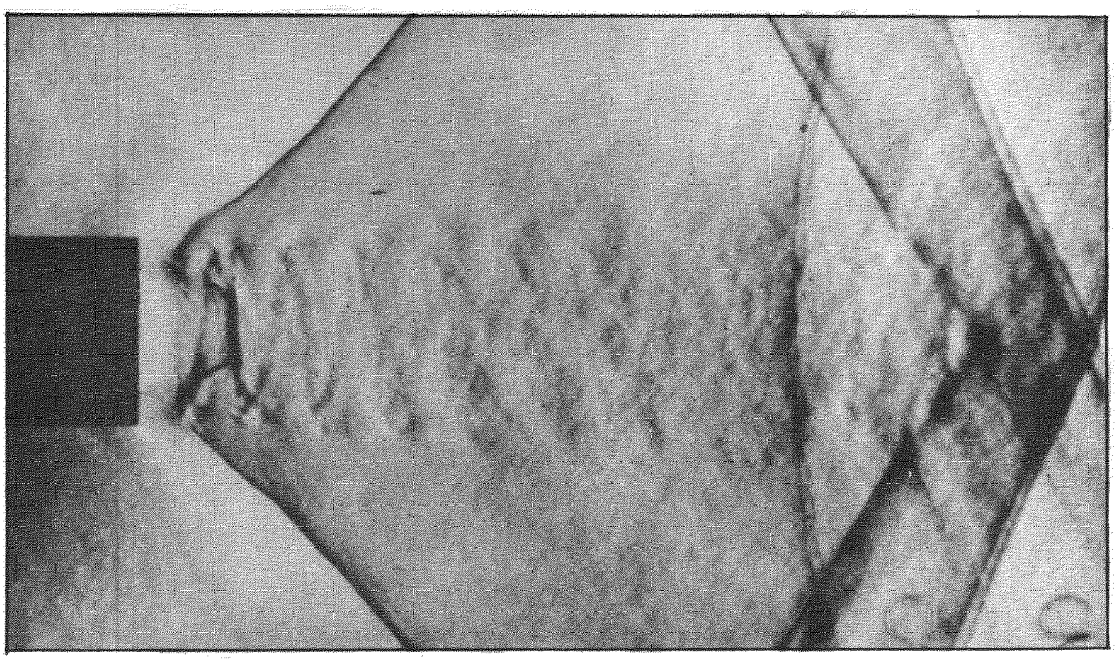

(b) Helical vortex shedding. $H_J / H_\infty = 1.31$

Fig.11. Schlieren photographs. $M_\infty = 1.2$. K.E. vertical

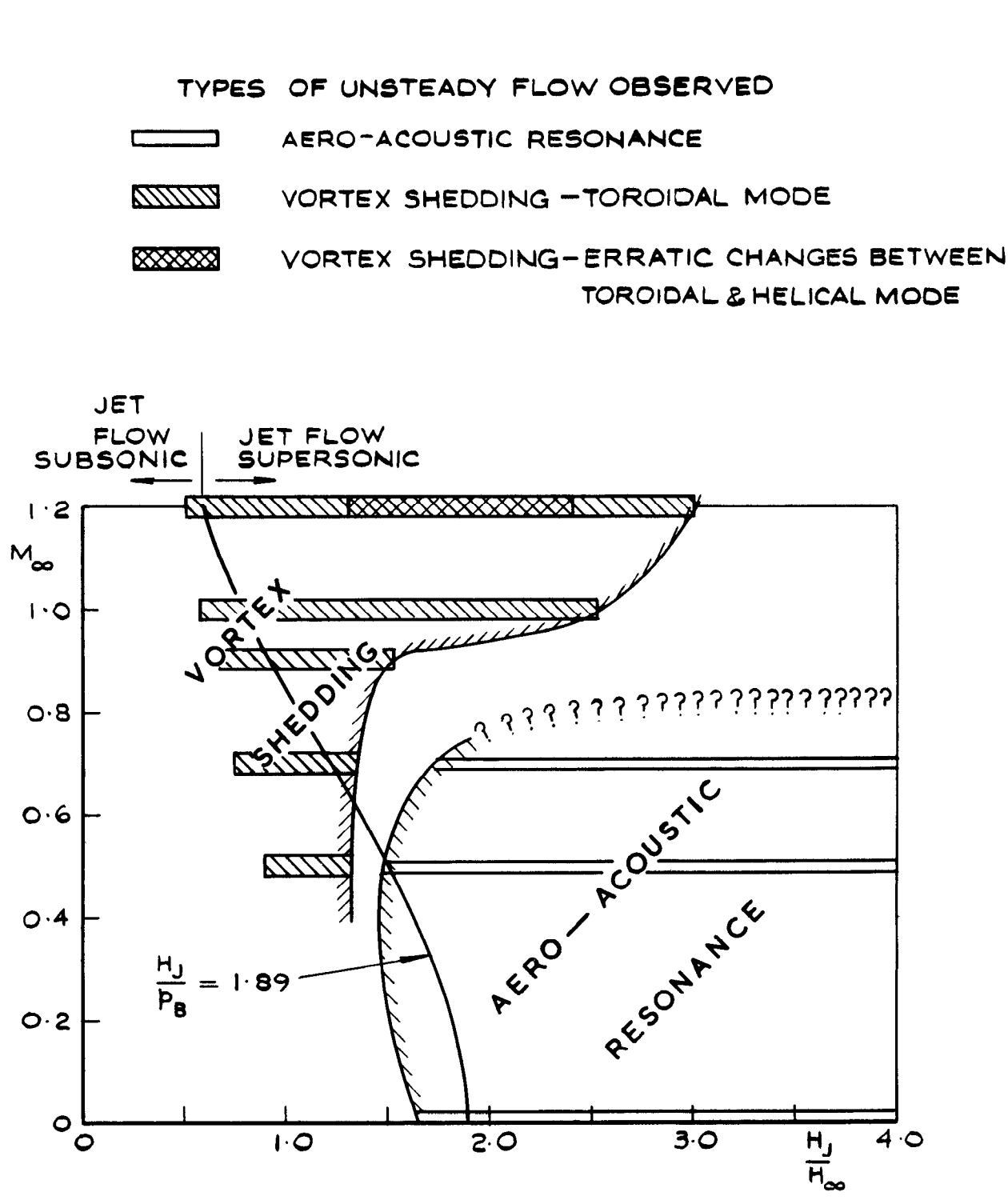

FIG. 12 CONDITIONS FOR DIFFERENT TYPES OF UNSTEADY FLOW IN JET

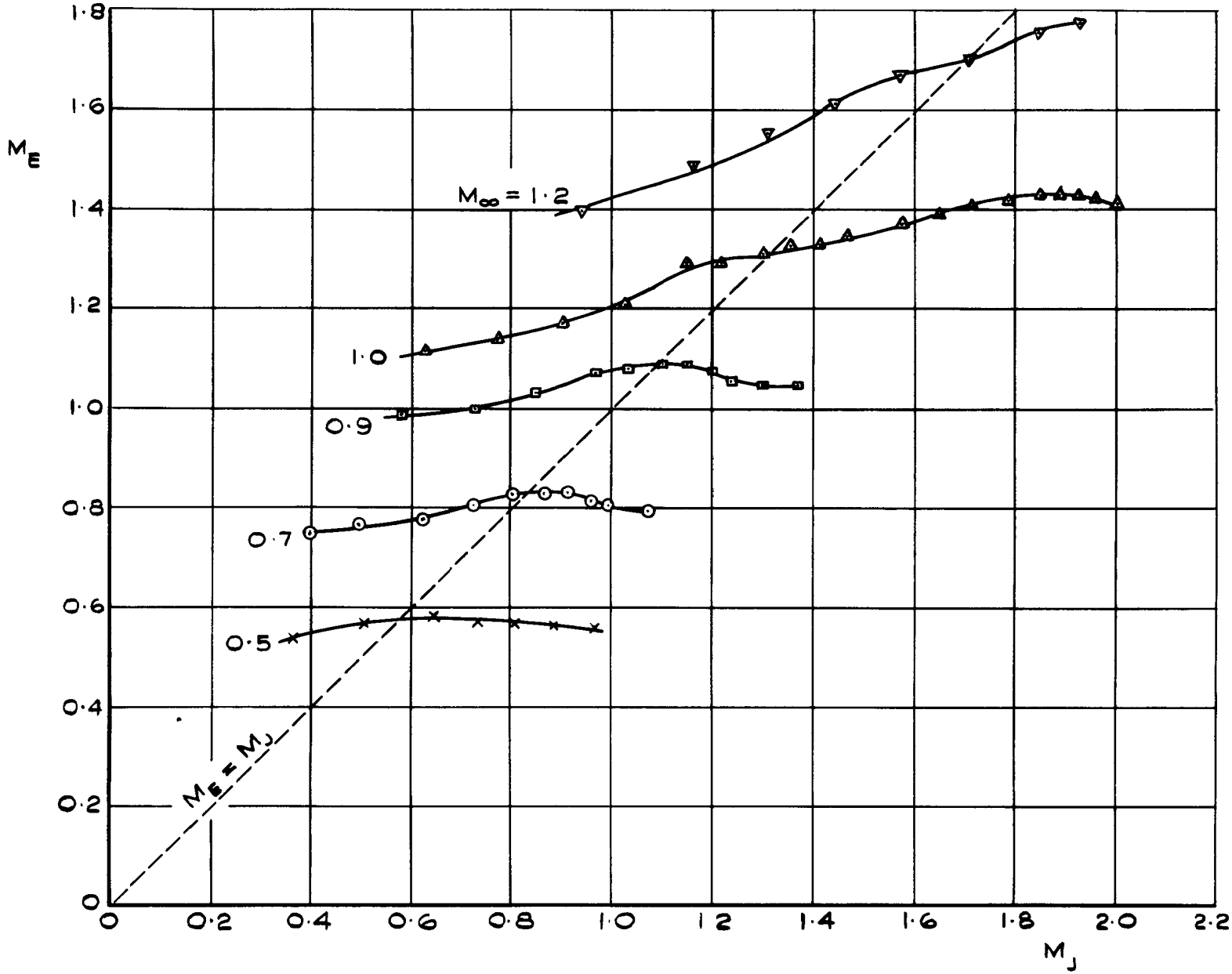

FIG.13 VARIATION OF M_E WITH M_J AND M_∞

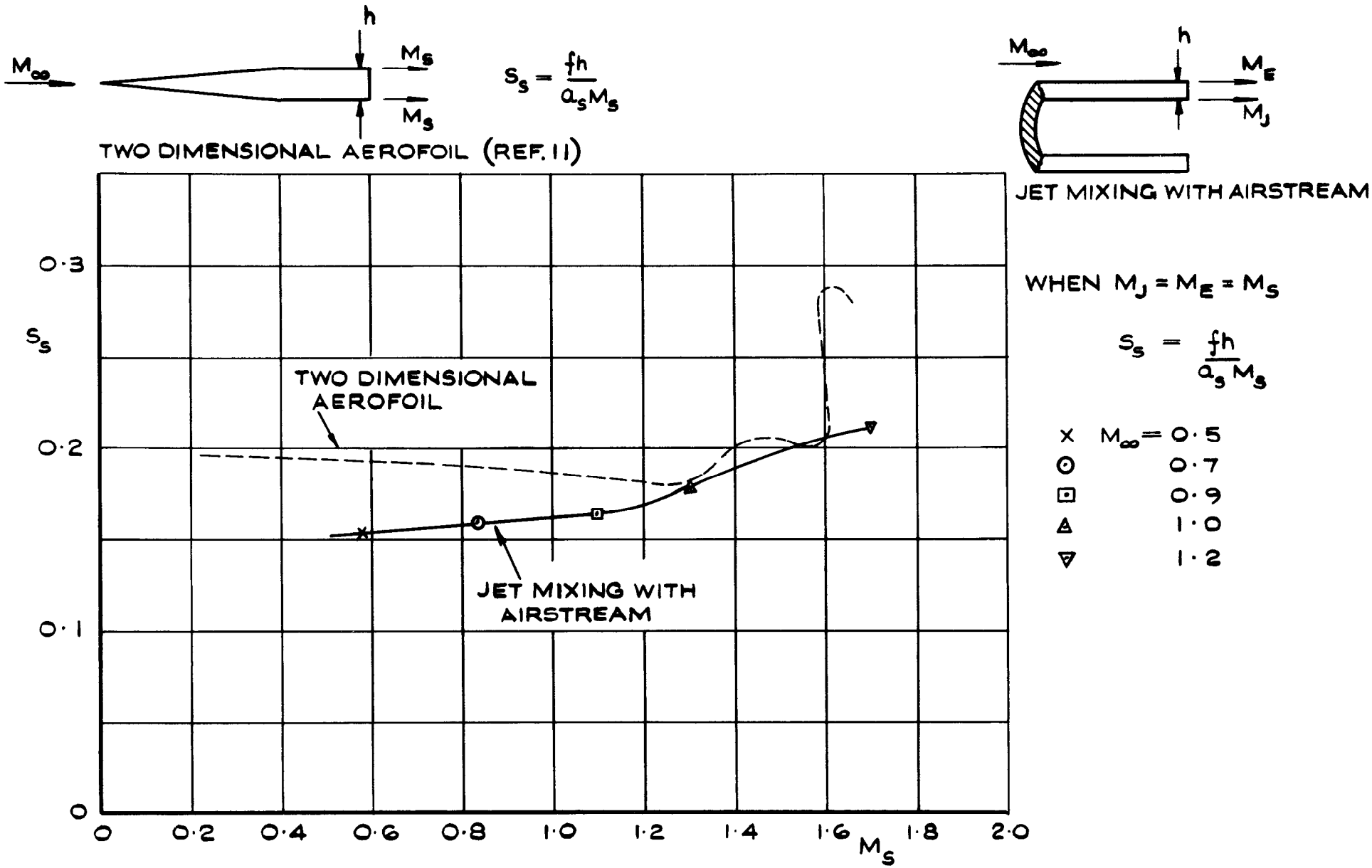

FIG.14 VARIATION OF STROUHAL NUMBER WITH MACH NUMBER WHEN $M_J = M_E$

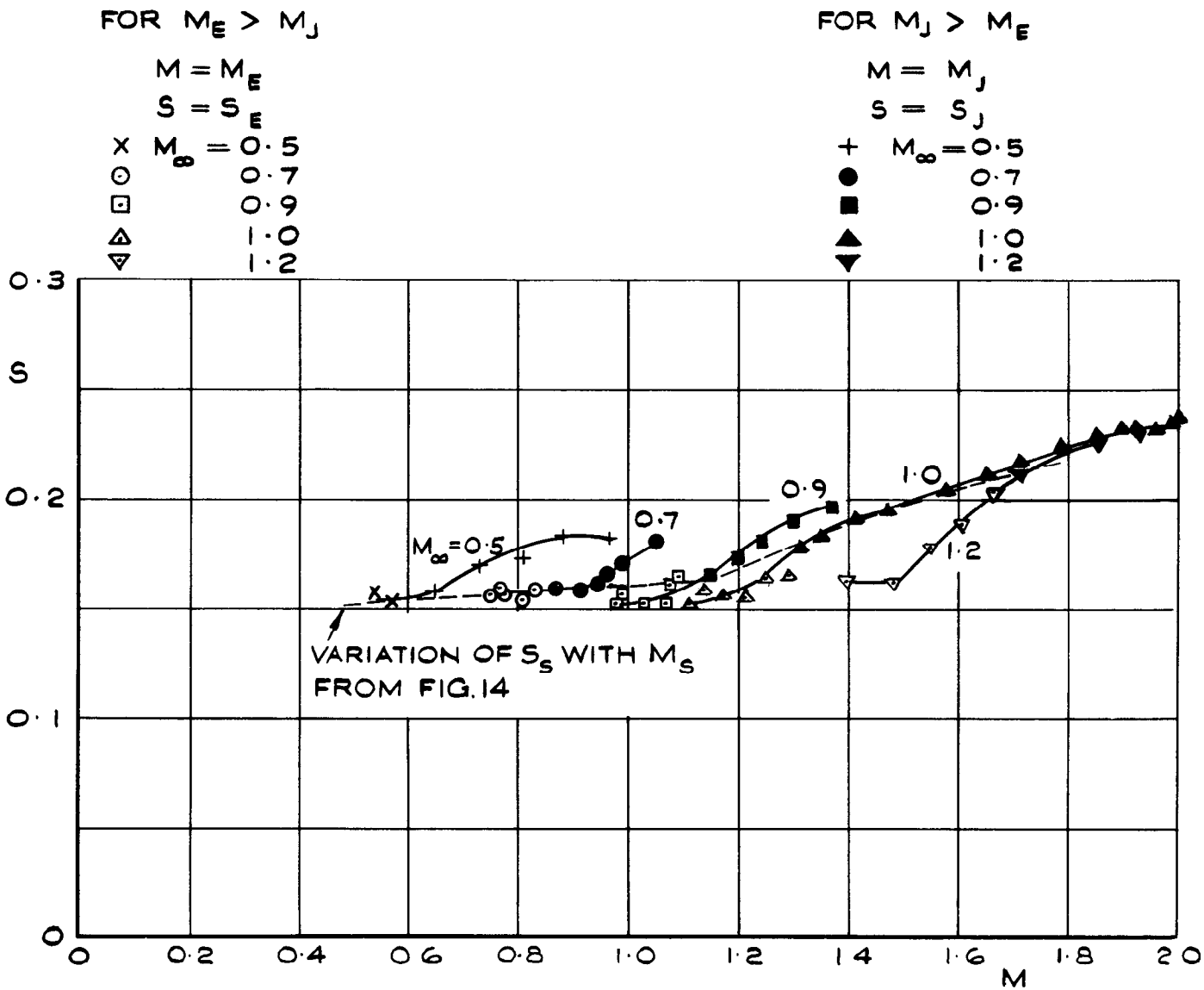

FIG.15 VARIATION OF STROUHAL NUMBER WITH MACH NUMBER $M_J \neq M_E$

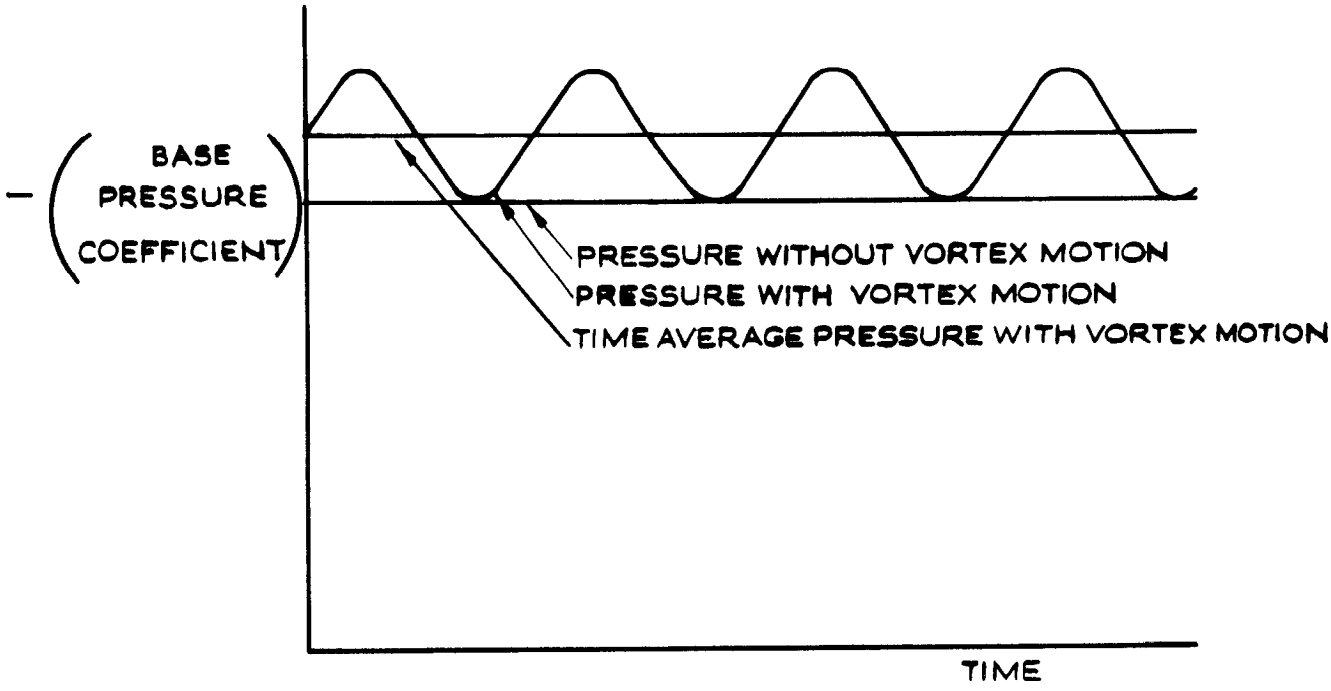

FIG.16 SUGGESTED COMPOSITION OF BASE PRESSURE

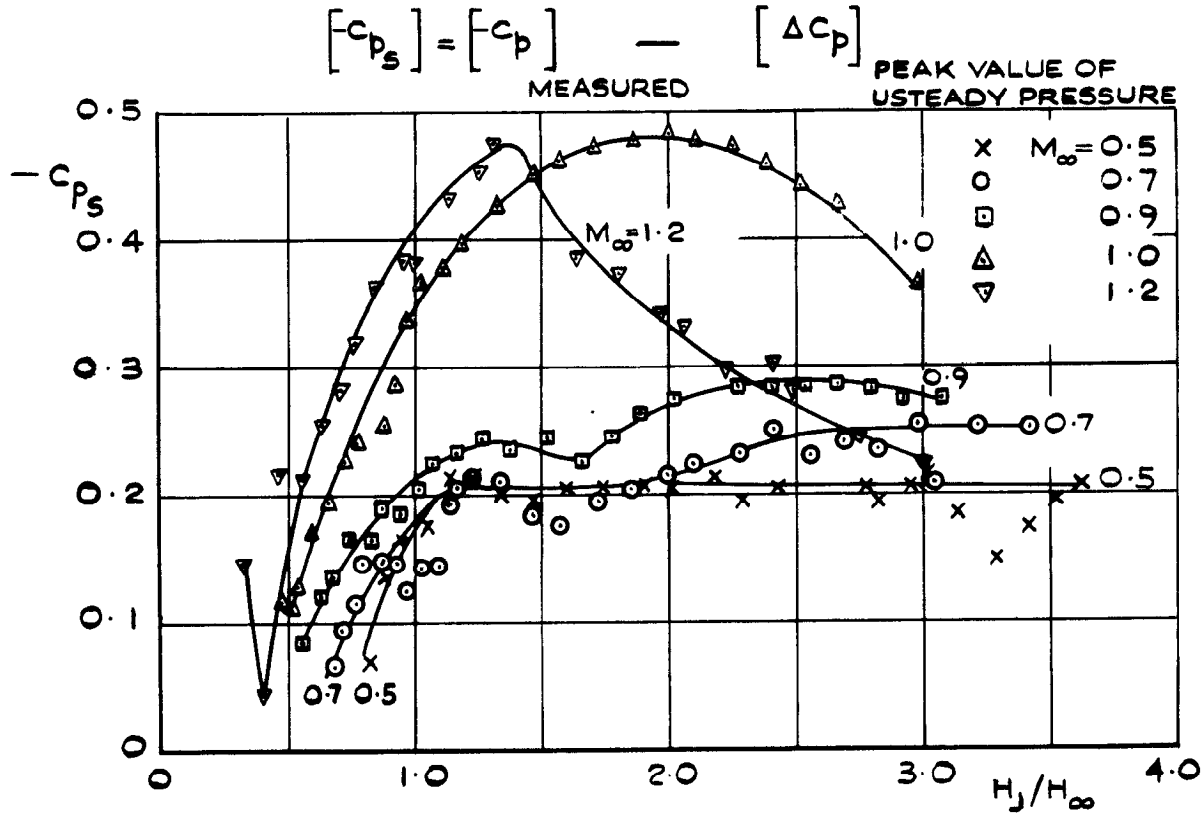

FIG.17 VARIATION OF "STEADY" BASE PRESSURE WITH MACH NUMBER AND JET PRESSURE RATIO (SEE PARA.4.2)

Printed in England for Her Majesty's Stationery Office by
the Royal Aircraft Establishment, Farnborough. Dd.125875.K.4.

A.R.C. C.P. No.903
August 1965
Rossiter, J.E.
Kurn, A.G.
WIND TUNNEL MEASUREMENTS OF THE EFFECT OF A JET ON THE TIME AVERAGE AND UNSTEADY PRESSURES ON THE BASE OF A BLUFF AFTERBODY

533.6.048.2 :
533.696.8 :
533.697.4 :
533.6.011.3

The time average and unsteady pressures have been measured on the base of a bluff afterbody, containing a single jet, in subsonic and transonic airstreams. Schlieren flash photographs have been used to investigate the mixing process.

It was found that over much of the range of investigation, the mixing of the jet with the external stream was dominated by a vortex motion analogous to the vortex street which occurs behind a bluff two dimensional body. This vortex shedding caused pressure fluctuations on the base of the model and had a significant effect on the time average base pressure.

A.R.C. C.P. No.903
August 1965
Rossiter, J.E.
Kurn, A.G.
WIND TUNNEL MEASUREMENTS OF THE EFFECT OF A JET ON THE TIME AVERAGE AND UNSTEADY PRESSURES ON THE BASE OF A BLUFF AFTERBODY

533.6.048.2 :
533.696.8 :
533.697.4 :
533.6.011.3

The time average and unsteady pressures have been measured on the base of a bluff afterbody, containing a single jet, in subsonic and transonic airstreams. Schlieren flash photographs have been used to investigate the mixing process.

It was found that over much of the range of investigation, the mixing of the jet with the external stream was dominated by a vortex motion analogous to the vortex street which occurs behind a bluff two dimensional body. This vortex shedding caused pressure fluctuations on the base of the model and had a significant effect on the time average base pressure.

A.R.C. C.P. No.903
August 1965
Rossiter, J.E.
Kurn, A.G.
WIND TUNNEL MEASUREMENTS OF THE EFFECT OF A JET ON THE TIME AVERAGE AND UNSTEADY PRESSURES ON THE BASE OF A BLUFF AFTERBODY

533.6.048.2 :
533.696.8 :
533.697.4 :
533.6.011.3

The time average and unsteady pressures have been measured on the base of a bluff afterbody, containing a single jet, in subsonic and transonic airstreams. Schlieren flash photographs have been used to investigate the mixing process.

It was found that over much of the range of investigation, the mixing of the jet with the external stream was dominated by a vortex motion analogous to the vortex street which occurs behind a bluff two dimensional body. This vortex shedding caused pressure fluctuations on the base of the model and had a significant effect on the time average base pressure.

DETACHABLE ABSTRACT CARDS

Published by
HER MAJESTY'S STATIONERY OFFICE
To be purchased from
49 High Holborn, London W.C.1
423 Oxford Street, London W.1
13A Castle Street, Edinburgh 2
109 St. Mary Street, Cardiff
Brazennose Street, Manchester 2
50 Fairfax Street, Bristol 1
35 Smallbrook, Ringway, Birmingham 5
80 Chichester Street, Belfast 1
or through any bookseller

C.P. No. 903

S.O. CODE No. 23-9017-3